Coral Reefs
https://doi.org/10.1007/s00338-025-02728-4

RESEARCH

Coping with ocean acidification: metabolic shifts in *Porites* corals from the Palau Archipelago

Keyla Plichon[1,2] · Marion Tredez[1,2] · Stéphane Roberty[3] · Marine Canesi[4] · Eric Béraud[2,5] · Eric Douville[4] · Didier Zoccola[2,5] · Eric Gilson[1,2] · Stéphanie Reynaud[2,5] · Paola Furla[1,2]

Received: 28 March 2025 / Accepted: 27 July 2025

Abstract Increased atmospheric CO_2 levels lead to ocean acidification, threatening coral reefs. However, certain coral species thrive in naturally acidified environments, offering unique opportunities to explore potential acclimatization or adaptation strategies. We assessed the physiological and biochemical parameters of *Porites* cf. *lobata*. colonies from control and acidified sites in the Palau Archipelago. Using a holistic approach, we compared markers related to trophic state, symbiotic state, physiology, energy storage, and redox status, along with calcification and oxidative metabolism. Our findings indicate that these colonies can acclimatize to low-pH conditions by utilizing CO_2 more effectively. The increased passive diffusion of CO_2 through their tissues enables them to maintain photosynthesis and calcification rates by reallocating energy that would typically go toward bicarbonate uptake. However, this energy reallocation cannot maintain skeleton density. Corals expend energy to elevate pH in the extracellular calcifying fluid, which is highly energy-demanding and reduces lipid reserves, potentially compromising long-term resilience. Despite the heightened energy production requirements, oxidative stress does not appear to worsen; the colonies exhibited lower antioxidant defenses and protein damage under low-pH conditions. The absence of metabolic suppression due to stable respiration rates and increased biomass suggests modifications in metabolic pathways, likely shifting toward a Warburg-like effect. These findings highlight the potential for some corals to tolerate near-future ocean acidification, the trade-offs associated with this resilience, and the potential for cascading effects on reef ecosystems. Further research should explore corals metabolic pathways as potential coping mechanisms.

Stéphanie Reynaud and Paola Furla have jointly supervised this work.

✉ Paola Furla
paola.furla@univ-cotedazur.fr

Keyla Plichon
keyla.plichon@gmail.com

Marion Tredez
marion.tredez@hotmail.fr

Stéphane Roberty
sroberty@uliege.be

Marine Canesi
marine.canesi@gmail.com

Eric Béraud
eberaud@centrescientifique.mc

Eric Douville
eric.douville@lsce.ipsl.fr

Didier Zoccola
zoccola@centrescientifique.mc

Eric Gilson
eric.gilson@univ-cotedazur.fr

Stéphanie Reynaud
sreynaud@centrescientifique.mc

[1] Institute for Research on Cancer and Aging, Université Côte d'Azur, CNRS, INSERM, Nice, France

[2] LIA-ROPSE, Laboratoire International Associé, Université Côte d'Azur - Centre Scientifique de Monaco, Monaco, France

[3] InBios-Animal Physiology, University of Liège, 4000 Liège, Belgium

[4] Laboratoire Des Sciences du Climat et de L'Environnement, LSCE/IPSL, CEA-CNRS-UVSQ, Université Paris-Saclay, 9119 Gif-Sur-Yvette, France

[5] Centre Scientifique de Monaco, 8 Quai Antoine Ier, Monaco, Monaco

Published online: 04 September 2025

Graphical Abstract

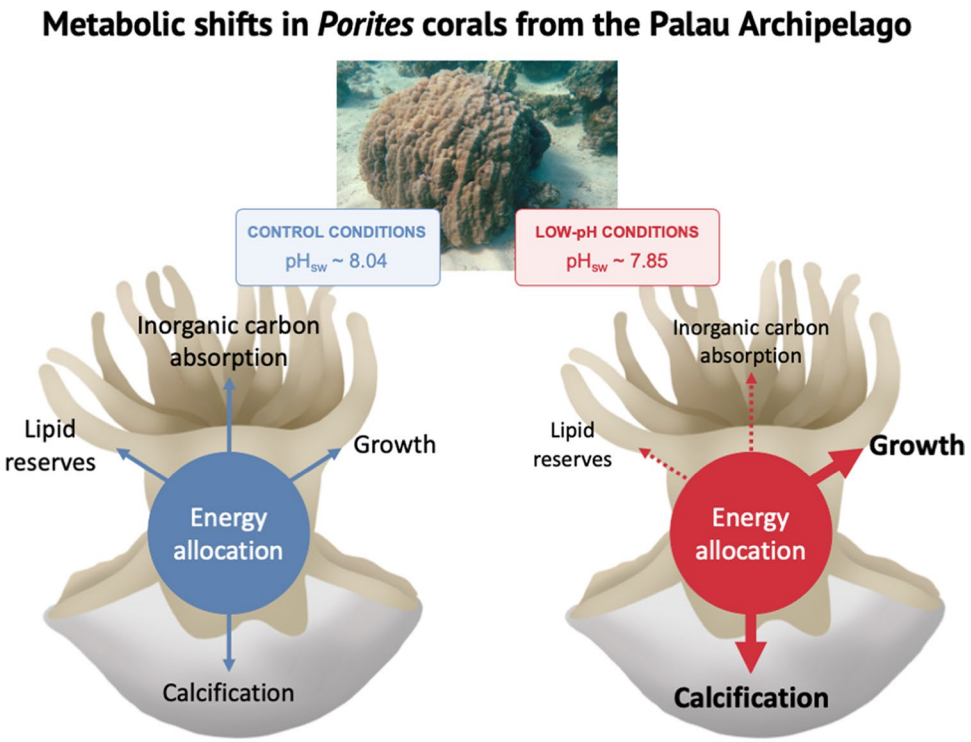

Keywords Carbonic anhydrase · Redox state · Calcification · Stable isotope · Lipids · Biomass

Introduction

Ocean acidification refers to changes in ocean chemistry caused by carbon dioxide (CO_2) uptake from the atmosphere due to human activities since the industrialization era. This process leads to an increase in dissolved inorganic carbon (DIC), changing seawater carbon equilibrium and resulting in a decline in pH and aragonite saturation state (Ω; (Orr et al. 2005; Gattuso and Hansson 2011; Gruber et al. 2019)). Studies on ocean acidification's effects on marine organisms have highlighted contrasting responses. Indeed, photosynthetic organisms may benefit from this increase in CO_2 (Koch et al. 2013), whereas calcifying organisms are considered vulnerable (Kroeker et al. 2013a, b; Leung et al. 2022), ultimately leading to changes in communities' structure and decreasing ecosystem resilience (Andersson et al. 2011; Kroeker et al. 2013a, b).

Scleractinian corals, with their aragonite skeletons produced through biomineralization in the calcifying fluid, are particularly susceptible to the effects of ocean acidification (Erez et al. 2011; Tambutté et al. 2011). The pH of the calcifying fluid, typically between 8.2 and 8.9 (McCulloch et al. 2012; Venn et al. 2019), is increased by the animal through calcium pumps (Ca^{2+}-ATPase) of the calicoblastic epithelium (Isa et al. 1980; Zoccola et al. 1999, 2004), resulting in inorganic carbon levels 1.5 to 2 times higher than in seawater and an increase in calcium carbonate Ω (DeCarlo et al. 2017). In addition, many scleractinian corals live in symbiosis with intracellular dinoflagellates from the family Symbiodinaceae, which plays a significant role in their survival in oligotrophic environments (Davies 1991; Muscatine et al. 1989; Wang and Douglas 1998). This partnership revolves around the metabolic exchange between the host and the symbiont. Indeed, the host supplies DIC to the symbiont through proton pumps and carbonic anhydrase, which act as a inorganic carbon concentrating mechanism that diffuses through animal tissues and allows photosynthesis by the symbiont (Brownlee 2009; Furla et al. 2000a, b; Weis et al. 1989). Photosynthesis products are then transported to the host to support vital functions such as growth or reproduction (Muscatine et al. 1984; Muscatine 1990; Davies 1991; Erez et al. 2011; Inoue et al. 2018). Previous studies have suggested that ocean acidification may not disrupt the symbiotic relationship of many coral species (Wall et al. 2014; Davies et al. 2018) or even increase primary productivity (Suggett et al. 2012; Biscéré et al. 2019). As ocean pH

decreases, corals must invest more energy in maintaining the pH of the calcifying fluid and maintaining their calcification rates (Allemand et al. 2004; Zoccola et al. 2004; Erez et al. 2011), possibly leading to increased energy requirements (Edmunds 2011) that might be mitigated by increased photosynthesis efficiency and product translocation. However, the mitigation might be efficient until a certain threshold is reached, and this additional energy demand could reduce their resistance to other environmental stressors (Cohen and Holcomb 2009; Pandolfi et al. 2011).

Much of the research on the effects of ocean acidification on corals is based on short-term CO_2 conditions in laboratory-controlled environments and, therefore, does not accurately reflect the long-term effects of ocean acidification in the wild (Fabricius et al. 2011). However, using naturally acidified sites as marine laboratories offers a unique and promising avenue for studying ocean acidification and the response of corals to the environment. These sites, which mimic near-future acidification scenarios, allow organisms to be studied under more realistic environmental conditions over broad temporal scales (González-Delgado and Hernández 2018; Hill and Hoogenboom 2022). Therefore, they provide invaluable insights into the acclimatization mechanisms and rapid evolutionary responses that allow organisms to live in low pH conditions.

The Palau Archipelago's naturally acidified site has recently received considerable attention. The reef's biological processes and water circulation patterns create a natural gradient established from the past 150–500 yr (measuring 8.05 to 7.84; Shamberger et al. 2014; Golbuu et al. 2016; Barkley et al. 2017; Canesi et al. 2024) that mimics predicted pH conditions by the year 2100 under RCP 8.5 scenario (IPCC 2019). The highly sheltered system in Nikko Bay (also known as Iwayama Bay) allows the seawater resident time being around 71 d (Golbuu et al. 2016), hence, representing a valuable opportunity to assess long-term acclimatization or local adaptation mechanisms. Indeed, coral coverage inside the bay was found to be high compared to outer reefs (van Woesik et al. 2012; Golbuu et al. 2016). Among the coral species that thrive, massive corals such as *Porites* (Link 1807) are found across the pH gradient. These corals, which are strictly associated with symbiotic dinoflagellates of the genus *Cladocopium* throughout the Pacific and Indian Oceans, are known to be slow-growing species, (about 1 cm per year; (Pätzold 1984; Linsley et al. 1999) and can live for hundreds of years (Stat et al. 2009; Bythell et al. 2018; Coward et al. 2020; Forsman et al. 2020; Smith et al. 2021). The genus *Porites* is known for producing annual density bands, which enable accurate growth measurements over time (Highsmith 1979; Flora and Ely 2003). Massive *Porites* corals have been shown to be more resistant to environmental perturbations such as temperature or pH changes than branching corals (Loya et al. 2001; Fabricius et al. 2011). Therefore, massive *Porites* corals are interesting candidates for understanding the long-term coping mechanisms and the possible adaptation to ocean acidification.

Here, we aimed to assess (1) how long-term exposure to low-pH conditions affects *Porites* cf. *lobata* colonies in the Palau Archipelago and (2) which cellular mechanisms allow their survival under low pH conditions. Using a holistic approach, we compared the physiology and metabolism of coral colonies from control and acidified sites. The studied markers are related to animal biomass, symbiotic state, energy storage, redox status, inorganic carbon source, calcification, and metabolism.

Material and methods

Site description and sampling

Coral colonies of massive *Porites* cf. *lobata* (Rivera et al. 2022) were sampled in Koror State (Republic of Palau, in Micronesia 7°17N, 134°15E) in January 2018. They have been sampled according to the marine research permit (RE-18-04), to the export permit from Republic of Palau (PW18-009) and to the CITES final import permit from France (FR1807512823-I).

The main islands are surrounded by a coral reef barrier and form a maze of small bays and semi-enclosed lagoons.

Table 1 Sampling site locations and environmental parameters

Site name	Site code	Lat	Long	SST (°C)	SSS (ppt)	TA (ppm)	DIC (µM)	pH (TS)	pCO_2 (µatm)	Ω_a
Malakal Island	CT 1	7°19.726 N	134°27.912 E	29.9	33.5	2116.5	1857.9	7.93	487.8	3.0
Uchelbeluu reef	CT 2	7°17.020 N	134°32.000 E	29.7	33.6	2170.6	1855.5	8.03	383.7	3.6
Ucheliungs	CT 3	7°18.687 N	134°30.122 E	30.1	33.4	2176.9	1770.7	8.16	255.6	4.6
Bukrrairong	AC 1	7°19.445 N	134°29.659 E	30.4	32.6	2023.4	1844.9	7.78	707.3	2.2
Semi-enclosed reef	AC 2	7°19.138 N	134°29.764 E	30.2	32.9	2042.4	1834.2	7.85	600.7	2.5
Ngeteklou	AC 3	7°19.342 N	134°29.458 E	30.1	32.7	2024.8	1820.7	7.84	606.5	2.4

Measured environmental parameters at each site are: sea surface temperature (SST), sea surface salinity (SSS), total alkalinity (TA), dissolved inorganic content (DIC), pH, partial pressure of carbon dioxide (pCO_2) and aragonite saturation state (Ω_a)

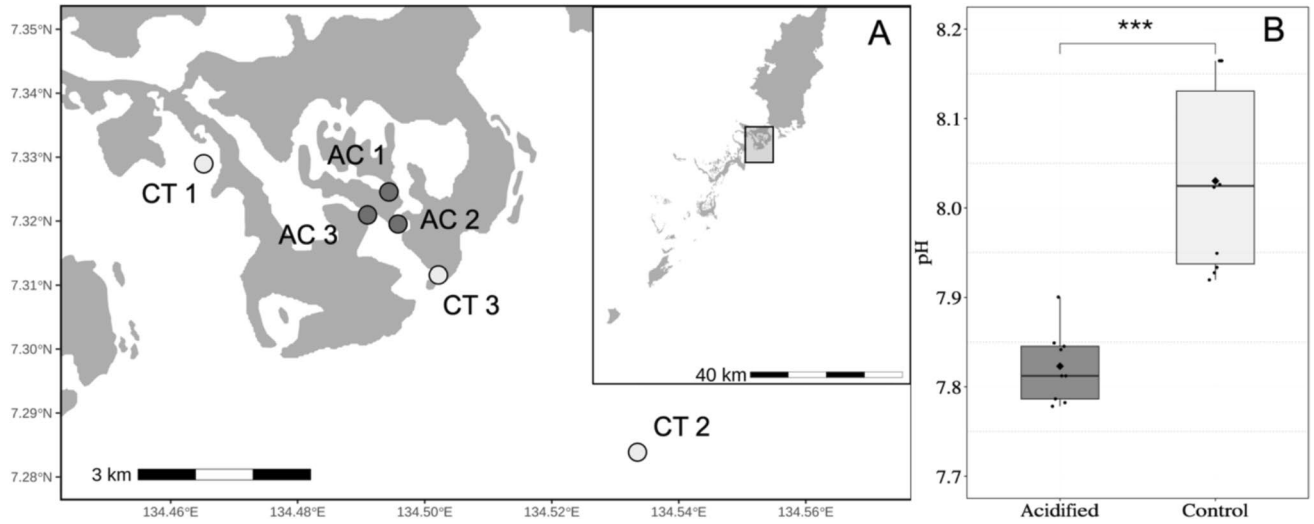

Fig. 1 Study area in the Palau Archipelago. Panel A represents the Koror studied area highlighted by the square zone in the insert) and the specific sampling sites with the control (CT, light gray) and acidified (AC, dark gray) location. Panel B shows the mean variation of pH between control (light gray) and acidified (dark gray) conditions. Significance:***: t-test, p-value ≤ 0.001

The relatively high acidity of Palauan coral reef seawater results from a combination of biological processes and circulation patterns within the reef system. Calcification, respiration, and dilution (mixing offshore source water with freshwater) appear to be the main factors driving changes in seawater chemistry. The environment found in Nikko Bay is relatively stable (diurnal pH variation inside and outside the bay: 0.05 to 0.25; Kurihara et al. 2021) and has been suggested to have been maintained for at least more than 500 years (Golbuu et al. 2016). The carbonate chemistry of Palauan reef seawater is significantly different from that of open ocean source water (Shamberger et al. 2014; Canesi et al. 2024).

Six sampling sites were selected, including three sites with pH ranging from 7.93 to 8.16, close to the current ambient pH hereafter referred as "control" (CT 1, CT 2, CT 3) and three low-pH sites, referred as "acidified" (AC 1, AC 2, AC 3), with pH ranging from 7.78 to 7.84 (Table 1; Fig. 1), corresponding to conditions predicted to occur in the tropical Pacific Ocean by the end of this century (IPCC 2018; IPCC 2019). The pH diel variability was analyzed in the bay by Kurihara and collaborators (2021) who found that pH at these sites ranges from 0 to 0.15 (Kurihara et al. 2021), both inside and outside the bay. At each site, two sets of fragments (10 g each) from 6 massive *Porites* cf. *lobata* colonies were sampled at approximately 5 m depth. Both sets were frozen in liquid nitrogen and stored at − 20 °C until analysis. The first set was used for biochemical and biomass analyses; the second was used for inorganic carbon source analysis.

Two massive *Porites* cf. *lobata* coral cores were collected from an open-ocean site (CT 3) and a semi-enclosed site (AC 2) on the southeastern coast of Palau during the Tara-Pacific expedition (Planes et al. 2019; Canesi et al. 2024) (Fig. 1). Cores were collected at 4 m depth using a hydraulic drill (Stanley®) with a 7 cm diameter corer. After drilling, a cement plug was placed in the hole to facilitate colony recovery. The two drilled skeletons were then used to measure colony growth and calcification parameters.

Porites cf. *lobata* fragments were also collected for photo-physiological measurements at CT 1 and AC 1 sites. At both sites, fragments from 5 colonies were sampled at depths between 5 and 8 m. The samples were then brought back on board the boat, where they were kept in a tank fed by a continuous flow of seawater. The photosynthetic and respiratory activities of the samples were measured on the day of collection using fluorometry and oximetry.

To determine the carbon isotopic composition of plankton, 10 L of seawater were collected and filtered through a pre-combusted 0.45 µm glass fiber filter, then dried until subsequent analysis.

pH_{sw} and total alkalinity measurements

Seawater was sampled at the control and acidic sites, and pH_{sw} (total scale with an uncertainty of ± 0.01; (Canesi et al. 2024) was measured using the meta-cresol purple indicator dye (Clayton and Byrne 1993; Dickson et al. 2007). The absorbances were measured using a Agilent Cary 60 UV–Vis spectrophotometer on board the *Tara*.

Seawater was also sampled at each site for total alkalinity (TA) and dissolved inorganic carbon (DIC). Measurements were performed at the SNAPSOCO2 facility of the Sorbonne University in Paris (France). Based on the

analysis of standard solutions, the external reproducibility for TA and DIC was ~ 3 µmol kg^{-1} (0.15%). TA and DIC values were used to calculate the complete carbonate chemistry at the sampling sites using the CO2SYS program (Lewis et al. 1998), with the carbonate species dissociation constant from Mehrbach et al., (1973), refitted by Dickson and Millero (1987), the borate and sulfate dissociation constants from Dickson (1990) and the solubility constant for aragonite from Mucci (1983). Calculated pHsw from TA and DIC dataset confirmed pH values obtained spectrophotometrically.

Sample preparation for inorganic carbon source analysis

Sampling glassware was pre-combusted at 480 °C for at least 6 h. Each coral was placed in a 100 ml beaker containing 10 to 20 ml of 0.45 µ-filtered seawater. Tissue was removed from the skeleton using an 'air pick' and homogenized using a Potter tissue grinder. The homogenate was then centrifuged at 2800 × g for 10 min at 4 °C to pellet most of the zooxanthellae. The supernatant was centrifuged at least 2 times for 10 min to pellet residual Symbiodiniaceae (Muscatine et al. 1989), transferred to 50 ml Pyrex tubes, and frozen (–20 °C) pending subsequent analysis. Symbiodiniaceae pellets were resuspended, washed 3 times with 0.45 µ-filtered seawater to avoid any tissue contamination, and frozen. Before isotopic measurements, tissue and Symbiodiniaceae samples were treated overnight with 0.05 M H_3PO_4 to remove carbonates (Muscatine et al. 1989) and freeze-dried. Organic carbon was analyzed by determining $\delta^{13}C$ values for coral tissue, Symbiodiniaceae, and plankton. Samples were homogenized by grinding, weighed into tin capsules, and analyzed using a dual-pumped Sercon 20–20 IRMS coupled to a Thermo EA1110 elemental analyzer, NC config, and a Carbosieve G column. Values are reported relative to the Pee Dee Belemnite standard in a delta notation (δ) expressed per mil (‰) using the formula below with R corresponding to (heavy isotope/light isotope). The precision for the isotopic analyses was 0.2 ‰.

$$\delta = \left[(\mathrm{R}sample/\mathrm{R}standard) - 1\right] \times 1000$$

Skeletal growth and calcification

The coral cores were scanned with a DISCOVERY CT750 high-definition Computed Tomography (CT) scanner at the DOSEO platform, CEA-Paris-Saclay, to reveal density changes associated with annual growth bands. The CT scans were used to measure linear extension rates (cm yr^{-1}), density changes (g cm^{-3}), and upward linear growth, following the protocols developed by Alaguarda et al. (2022). Linear extension and density were measured along three parallel growth axes (n = 3) on both cored colonies (i.e., extracted from the control and acidified sites) by measuring the distance between successive low-density bands over the last 6 yr of growth (2010–2016), excluding the tissue layer (i.e., the year 2017), to minimize potential seasonal or structural biases, as described in Canesi et al. (2024). The annual coral calcification rate (g cm^{-2} yr^{-1}) was calculated as the product of the linear extension rate and the skeletal density. The uncertainties of the linear extension rate and the density measurements were 4 and 2% (2σ), respectively. The calcification rate uncertainty was calculated as the square root of the sum errors of the density and linear extension and was equal to 4.5% (2σ).

Animal and symbiodiniaceae biomasses

A fragment of approximately 1 cm^2 was used for biomass analyses from the collected samples. Coral fragments were incubated in a sodium hydroxide solution (1N) as described by Zamoum and Furla (2012). After incubation, aliquots of the lysate were used to count Symbiodiniaceae cells using disposable counting chambers (Kova® Glasstic® Slide, USA). The Bradford protein assay (B6916, Sigma-Aldrich) was used to determine the animal protein concentration (Bradford 1976). The aluminum foil technique was used to measure the surface area of the remaining coral skeleton (Hoegh-Guldberg 1988). Animal biomass was expressed as mg of protein per surface (mg cm^{-2}), while symbiont biomass was expressed as the number of cells per mg of animal protein (cells mg^{-1}).

Biochemical markers

Total lipid and cytosolic extractions

Total lipid extraction was performed with a modified version of McLachlan et al. (2020). A fragment of approximately 10 cm^2 was incubated in 10 mL of a mixture of chloroform:methanol (2v:1v) and butylated hydroxytoluene (50 mg L^{-1}). After one hour, the extracts were centrifuged at 1 600 g for 5 min and stored in a clean glass container until purification. Extracts were then purified with a 0.88% KCl solution in a glass separatory funnel. The organic phase was then evaporated, and the lipids were resuspended in 1 mL of chloroform:methanol (2v:1v).

Total cytosolic extraction steps were performed under constant cooling (4 °C). Upon extraction, fragments of approximately 5 cm^2 were ground to powder and stored at

− 20 °C. Soluble cytoplasmic proteins and carbohydrates were extracted by resuspending the powder in a hypo-osmotic lysis buffer consisting of 25 mM 2-[4-(2-hydroxyethyl)piperazin-1-yl]ethanesulfonic acid, 5 mM $MgCl_2$, 5 mM 4-dithiothreitol, 5 mM ethylenediaminetetraacetic acid, 2 mM phenyl methyl sulfonyl fluoride, protease inhibitor cocktail (1 µL mL^{-1}) and anti-phosphatase (10 µL mL^{-1}) at pH 7.5 (ThermoScientific). The lysates were centrifuged at 12 000 g for 5 min, and only the supernatant containing the animal cytosoluble fraction was collected. The supernatant was stored at − 20 °C until analysis. The aliquots obtained were used for carbonic anhydrase activity, total antioxidant capacity, protein carbonylation, and carbohydrate analyses. The Bradford protocol was followed to determine the protein concentration of the supernatant using bovine serum albumin (BSA) solution as standard.

Carbonic anhydrase activity

Animal carbonic anhydrase (CA) activity was determined according to Weis et al. (1989). Briefly, animal carbonic anhydrase activity was measured using CO_2 as a substrate and following the pH decrease due to the hydration of CO_2 to form HCO_3^- and H^+. Assays were performed in a chamber containing 100 µg of protein diluted in Veronal buffer (25 mM NaVeronal, 5 mM EDTA, 5 mM DTT, and 10 mM MgSO4; pH 8.2). The carbonic anhydrase activity was normalized to minutes and mg of animal proteins (AU min^{-1} mg^{-1}).

Total antioxidant capacity

The total antioxidant capacity was tested using a modified version of Naguib's (2000) total oxidant scavenging capacity (TOSC) assay. Cytosoluble extracts were diluted in a phosphate buffer to obtain protein concentrations between 0.01 and 0.045 mg mL^{-1} in the reactive medium. The fluorescence signal was obtained by the oxidation of fluorescein (224 mM) by 2,2′-azobis(2-methylpropionamidine) dihydrochloride (600 mM). Calibration was performed with 6-hydroxy-2,5,7,8-tetramethyl-1-chroman-2-carboxylic acid (Trolox, 1.02 mM). The fluorescence decay was recorded using a spectrofluorometer (SAFAS, Monaco) at an excitation/emission wavelength of 520/495 nm for 1 h. Relative antioxidant activities of protein samples were measured by comparison with Trolox standard, and results were expressed as µmol Trolox equivalents normalized to mg of animal protein (eq Trolox µmol mg^{-1}).

Protein carbonylation

Protein carbonylation is a proxy for protein damage caused by oxidative stress. Carbonylated protein contents were measured using ELISA assay followed by spectrophotometric quantification according to Buss et al. (1997). Cytosolic proteins (0.5 µg $µL^{-1}$) were derivatized with a dinitrophenylhydrazine (DNP) solution (10 mM in 6 M guanidine hydrochloride and 0.5 M potassium phosphate, pH 2.5). Antibody against the DNP component (anti-rabbit DNP; 1:2000) was used as the primary antibody, and a Goat anti-rabbit IgG peroxidase conjugate (1:3000) was used as secondary antibody. A standard curve of reduced and oxidized BSA was included in each microplate. Derivatized proteins were finally detected by incubating the microplate for 20 min at room temperature with a reaction solution (0.6 mg mL^{-1} o-phenylenediamine, hydrogen peroxide (1:2500), 50 mM Na_2HPO4, 24 mM citric acid). The absorbance was read at 490 nm with a spectrophotometer (SAFAS, Monaco). Carbonyl contents were expressed as nmol per mg of animal protein (nmol mg^{-1}).

Total carbohydrate content

The carbohydrate content was determined using a modified phenol–sulfuric acid method described by Masuko et al. (2005). Briefly, 30 µL of each sample were deposited in a 96-well plate with 100% sulfuric acid and incubated in the dark for 15 min at 90 °C. After 15 min, 5% phenol was added to each sample, and the reaction was incubated for 5 min at room temperature. The absorbance was read at 490 nm using a spectrofluorometer (SAFAS, Monaco). The standard curve was prepared with known concentrations of D-glucose (from 0 to 24 mg mL^{-1}), and values were expressed as mg of carbohydrate per mg of animal protein (mg mg^{-1}). A detailed protocol can be found at protocols.io (Plichon and Furla 2024a).

Total lipids content

Lipid quantification was performed using a modified version of the sulfo-phospho-vanillin method described in Cheng et al. (2011). Briefly, 150 µL of the sample were evaporated in an individual hemolysis glass tube at 90 °C for 30 min. Then, 150 µL of concentrated sulfuric acid were added to the dried sample and incubated at 90 °C for 20 min. Finally, 100 µL were transferred to a 96-well plate, and the background absorbance was determined with a spectrophotometer at 540 nm (SAFAS, Monaco) before the addition of a reagent solution containing 17% phosphoric acid and 2 mg mL^{-1} of vanillin. The plate was then incubated at 37 °C for 15 min, and the absorbance was determined at 540 nm.

The final concentration was determined using a cholesterol standard curve. The lipid content was normalized to mg of animal protein (mg mg^{-1}). The detailed protocol is available on protocols.io (Plichon and Furla 2024b).

Photosynthesis and respiration

Chlorophyll fluorescence measurements

The chlorophyll fluorescence parameters of the coral fragments were measured on board Tara using a diving-PAM chlorophyll fluorometer (Walz GmbH, Germany). Prior to measurement, samples were kept in a 30 L tank, which was sheltered from direct sunlight and supplied with water continuously pumped from a depth of a few meters below the sea surface. Measurements were always taken with the fiber optic of the diving-PAM positioned 0.5 cm above the sample. After a 30-min dark adaptation period, the maximal photochemical quantum yield was measured with gain (G) and attenuation (D) set to 4 and 1, respectively. The initial fluorescence level (F0) was determined by applying weak modulated pulses of red measuring light (MI = 12). A 0.8 s saturating pulse of actinic light (SI = 12; ≈ 3000 µmol photon m^{-2} s^{-1}) was then applied to estimate the maximum fluorescence level (Fm). The maximum photochemical quantum yield was calculated as (Fv/Fm), where Fv = Fm-F0.

Oxygen exchange measurements

Photosynthesis and respiration rates were measured using a FireSting O_2 optical oxygen sensor (Pyro Science, Germany) mounted in a double-walled acrylic chamber with an internal volume of 70 mL. A continuous flow of water from a 15-L tank maintained at 30 °C was used to keep the temperature in the chamber constant. This corresponded to the average temperature at the various sampling sites. The optode was calibrated against oxygen-saturated seawater (100% air saturation) and sodium dithionite-saturated seawater (0% oxygen saturation). Actinic light was provided by LED light sources (light temperature 10 000 °K). After 7 min of dark acclimation, the oxygen concentration was monitored for 5 min at different light levels (0, 95, 140, 267, 530, and 1068 µmol photon m^{-2} s^{-1}). Respiration and net photosynthesis rates were then derived from the linear regression slope of the variation in oxygen concentration over the incubation time. Data were then normalized by the surface area of coral fragments using the wax dipping method described in Stimson and Kinzie (1991).

Data analysis

Raw data is available in Zenodo (Plichon et al. 2024). To analyze the results of the biochemical markers, linear regression analysis was performed for each marker, and a comparison between the control and acidified sites was displayed in boxplots. The variance distribution for each variable was presented as boxplots generated using the R (v.4.3.1) package ggplot2 (v.3.4.4). The rationale for these representations is to identify potential continuous relationships between the measured parameter and pH while summarizing the main differences between the control and acidified sites. The Shapiro–Wilk test assessed the normal distribution of the raw data, while the Bartlett test assessed homoscedasticity. A parametric t-test or a nonparametric Wilcoxon–Mann–Whitney test was performed to compare unpaired samples from control and low-pH conditions. Pearson (parametric) or Spearman (non-parametric) correlation tests were performed to assess the correlation between the biochemical markers and pH.

Results

Environmental assessment of the studied area

The control and low-pH sites demonstrate clear differences in seawater physico-chemical parameters. On average, pH at the control sites is 8.04 ± 0.12, while the inshore low-pH site records a lower average pH of 7.82 ± 0.04. Correspondingly, mean aragonite saturation state (Ω_arg) is higher at the control sites (3.73 ± 0.81) than at the low-pH site (2.37 ± 0.15).

The low-pH site also exhibits slightly elevated seawater temperatures (30.23 ± 0.15), reduced salinity (32.73 ± 0.15), and lower total alkalinity (2030.20 ± 10.59) compared to the control site. However, the minor temperature difference does not fully explain the disparity in aragonite saturation states between the inshore and offshore reefs (Shamberger et al. 2014). While total dissolved inorganic carbon (DIC) remains comparable, pCO_2 levels are significantly higher at the acidified sites (638.17 ± 59.94) than at the control sites (375.70 ± 116.31).

These observed conditions at the sampling sites are consistent with present-day oceanic trends and align with IPCC projections, with the low-pH site's pH resembling RCP 8.5 scenarios and its pCO_2 values corresponding to those predicted under RCP 4.5 (IPCC 2019).

Dissolved inorganic carbon source

The $\delta^{13}C$ of the animal tissues obtained from the acidified sites were more negative than for the control site: − 15.70 ‰ ± 0.10 ‰ vs. − 13.46 ‰ ± 0.20 ‰ (Fig. 2A, Student t-test, *p*-value = 0.0004).

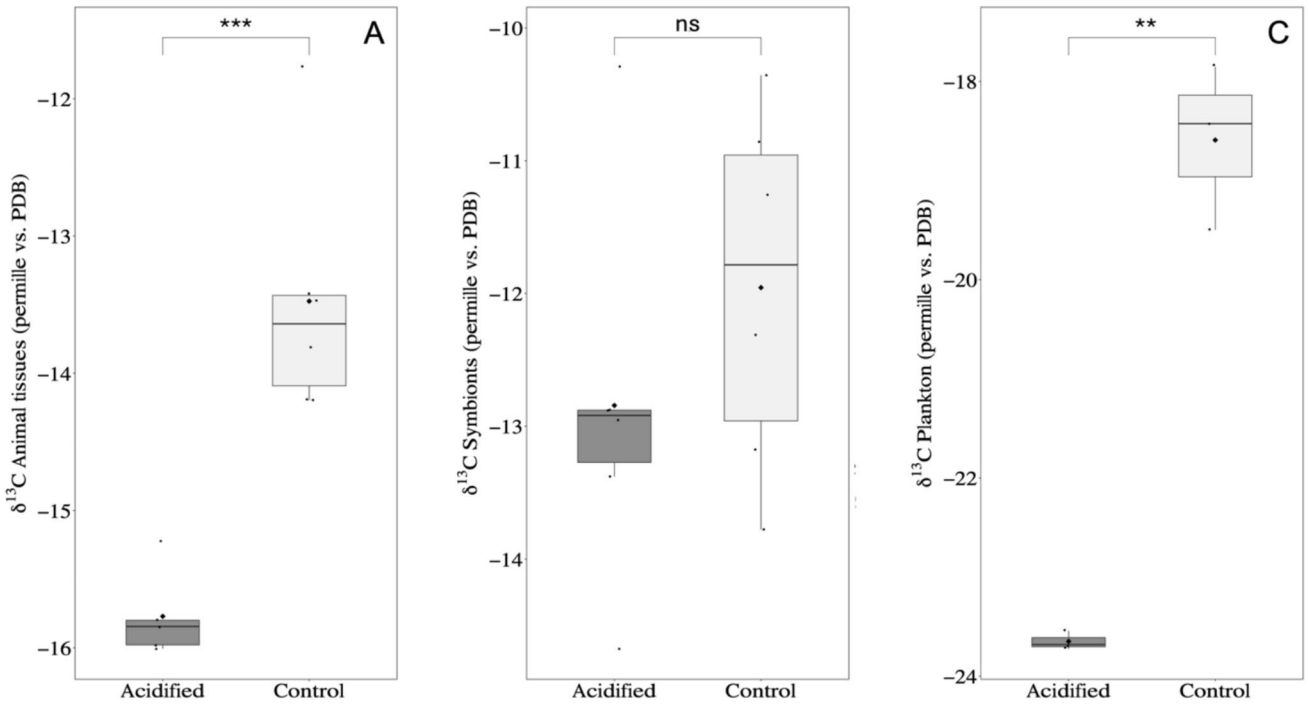

Fig. 2 Carbon isotopic composition of *Porites* cf. *lobata* colonies and plankton. $\delta^{13}C$ composition in *Porites* cf. *lobata* animal tissues (**A**), symbionts (**B**), and plankton (**C**) from colonies sampled at control (light gray; n = 6) and acidified (dark gray; n = 6) sites. Dots correspond to values measured in each colony; diamonds represent the mean of each site. Significance: n.s > 0.05; ** ≤ 0.01; *** ≤ 0.001

Table 2 Calcification rate and skeleton properties measured in skeleton cores from *Porites* cf. *lobata*. colonies

	Growth parameters		
	Extension (n = 3)	Density (n = 3)	Calcification (n = 3)
	cm yr^{-1}	g cm^{-3}	g cm^{-2} yr^{-1}
Control site	1.40 ± 0.06^{a}	1.51 ± 0.06^{a}	2.11 ± 0.13^{a}
Acidified site	1.54 ± 0.06^{b}	1.18 ± 0.05^{b}	1.82 ± 0.11^{a}

Averaged growth parameters (linear extension rate, skeletal density, calcification rate from 2010 to 2016) of the two massive *Porites* cf. *lobata* coral colonies extracted from the control (pHsw = 8.03) and acidified (pHsw = 7.85) sites in Palau. Growth parameters are expressed as the mean of three measurements for each of the studied colonies. Letters indicate significant differences between sites (Student's t-test, $P < 0.05$)

For the symbionts, the mean $\delta^{13}C$ was not significantly different: − 12.82 ‰ ± 0.31 ‰ vs. − 11.98 ‰ ± 0.32 ‰ (Fig. 2B, Student's t-test, *p*-value = 0.3). Finally, there was a significant difference between acidified (− 23.65 ± 0.07 ‰) and control (− 18.59 ± 0.6 ‰) sites for plankton (Fig. 2C, Welch t-test, *p*-value < 0.01). In low-pH conditions, animal tissues $\delta^{13}C$ (− 15.70 ‰ ± 0.10 ‰) is closer to the symbionts' values (− 12.82 ‰ ± 0.31 ‰) than plankton (− 23.65 ± 0.07 ‰).

Skeletal growth and calcification

Table 2 presents the averaged skeletal density, linear extension, and calcification rates from 2010 to 2016. While calcification remained unchanged between control and acidified sites, linear extension and skeletal density differed. Indeed, linear extension was approximately 10% higher in low-pH conditions than control, with a reduced skeleton density by approximately 21%.

Biochemical markers

Animal and symbiotic biomasses

Figure 3A shows a negative correlation between the animal biomass and the pH of the experimental sites (Spearman correlation test, r = − 0.517, *p*-value = 0.002). The animal biomass was almost twice as low in *Porites* cf. *lobata* colonies at control sites as in those at acidified sites (respectively of 1.23 ± 0.17 mg of protein cm^{-2} and 1.99 ± 0.11 mg of protein cm^{-2}; Student's t-test, *p*-value < 0.001; Fig. 3B). A positive correlation was also found between symbiont density and pH (Fig. 3C, Pearson correlation test, r = 0.526, *p*-value = 0.001). Still, the symbiont density did not differ significantly between the control and acidified sites (Fig. 3D, Wilcoxon–Mann–Whitney test, *p*-value = 0.2).

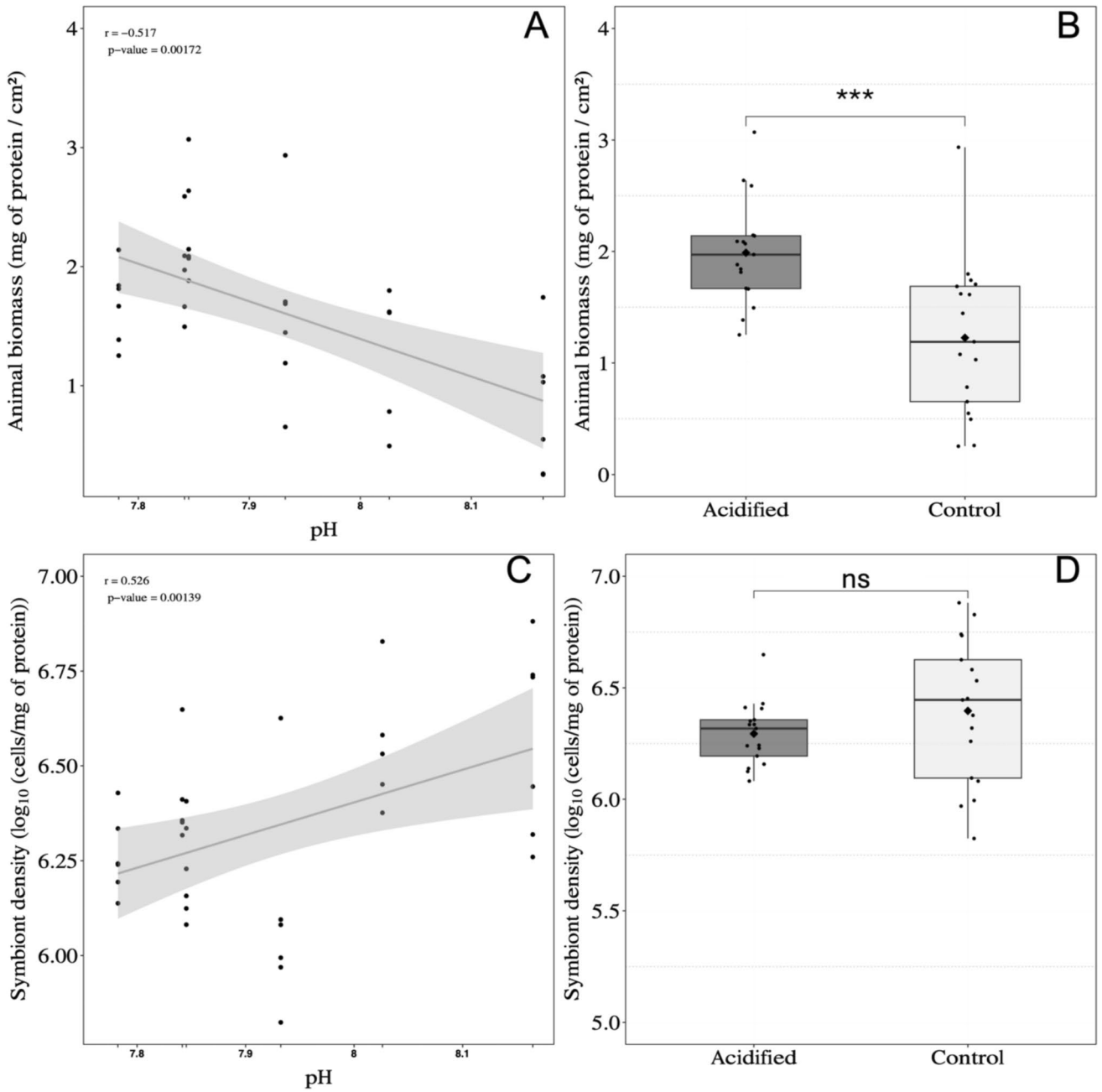

Fig. 3 Animal biomass and symbiont density from *Porites* cf. *lobata* colonies. Linear regression between animal biomass (**A**) or symbiont density (**C**) and pH, with the confidence interval colored in gray. Dots correspond to values measured in each colony. Animal biomass (**B**) and symbiont density (**D**) at control (light gray; n = 17) and acidified (dark gray; n = 17) sites are represented by boxplot; diamonds represent the mean of each site. Significance: n.s > 0.05; *** ≤ 0.001

Carbonic anhydrase activity

A positive correlation between carbonic anhydrase activity and pH was observed (Fig. 4A, Spearman correlation test, r = 0.516, *p*-value = 0.007). Carbonic anhydrase activity in the control condition was twice as high as in the low-pH condition (respectively (118.09 ± 15.99 AU min^{-1} and 58 ± 8.15 AU min^{-1}; Wilcoxon–Mann–Whitney test, *p*-value = 0.001; Fig. 4B).

Redox status

The redox status of colonies sampled from control sites was significantly different from those from colonies sampled

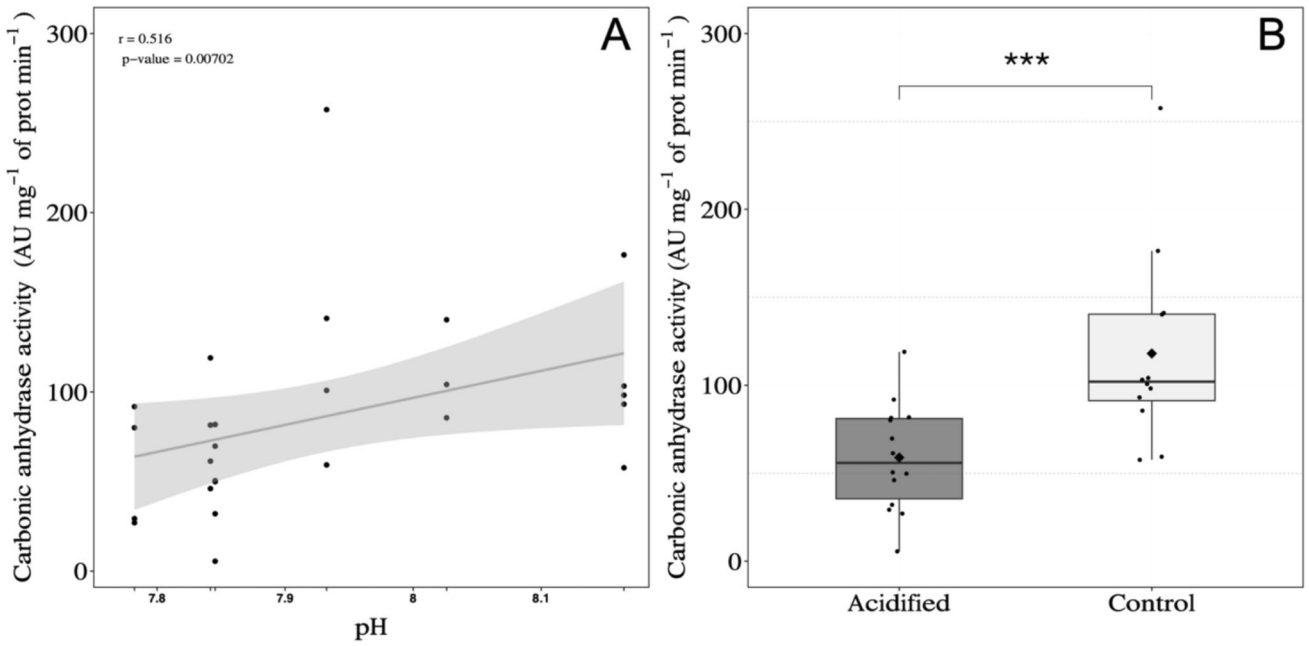

Fig. 4 Carbonic anhydrase activity of colonies of *Porites* cf. *lobata* colonies. Linear regression (**A**) between carbonic anhydrase activity and pH, with the confidence interval colored in gray. Dots correspond to values measured in each colony. Carbonic anhydrase activities (B) measured at control (light gray; n = 17) and acidified (dark gray; n = 17) sites are represented by boxplot; diamonds represent the mean of each site. Significance: *** ≤ 0.001

in acidified sites (Fig. 5). A significant positive correlation was found between total antioxidant capacity or carbonylated protein content and pH (Spearman correlation test, p-value < 0.0001; Fig. 5A, C). In addition, Fig. 5B shows that the total antioxidant capacity in control conditions was twice as high as in low-pH conditions (respectively 16.55 ± 1.78 and 7.85 ± 0.71 Eq. 1 µM Trolox m g^{-1} of protein; Welch t.test, p-value = 0.0002). Besides, carbonylated protein content was almost twice as high in control sites as in acidified sites (respectively 34.19 ± 2.58 and 59.56 ± 4.02 nmol mg^{-1} of protein; Welch t.test, p-value < 0.0001; Fig. 5D).

Total carbohydrate and lipid content

No correlation between total carbohydrate content and pH was found (Spearman correlation test, r = − 0.03, p-value = 0.9; Fig. 6A) and total carbohydrate content remained unchanged between conditions (Wilcoxon–Mann–Whitney, p-value = 0.8; Fig. 6B). However, a positive correlation was found between total lipid content and pH (Fig. 6C, Spearman correlation test, r = 0.436, p-value < 0.01). Total lipid content was statistically different between conditions, as lipid levels at control sites were twice as high as those at acidified sites (2.45 ± 0.39 mg mg^{-1} of protein and 1.25 ± 0.22 mg mg^{-1} of protein, respectively; Wilcoxon–Mann–Whitney, p-value = 0.013; Fig. 6D).

Photosynthesis and respiration

The acidified environment unaffected net photosynthesis (Fig. 7A, Student's t-test, p-value = 0.5), respiration (Fig. 7B, Student's t-test, p-value = 0.05), and effective quantum yield (Fig. 7C, Student's t-test, p-value = 0.2).

Discussion

This study investigated the adaptive mechanisms of *Porites* cf. *lobata* corals to local acidification in the Palau archipelago. Despite maintaining key physiological functions such as symbiont density, photosynthesis, respiration, carbohydrate content, and calcification, corals in acidified sites exhibited shifts in cellular pathways. Notably, differences in inorganic carbon sources were observed highlighted by reduced carbonic anhydrase activity in low-pH conditions. Corals also displayed decreased lipid content and redox status but increased animal biomass, suggesting potential metabolic adjustments to acidification.

Porites cf. *lobata*. becomes more efficient at utilizing CO_2 in lower pH conditions

Under control conditions, the dissolved inorganic carbon in oceanic seawater (at around pH 8.0) is mainly bicarbonate

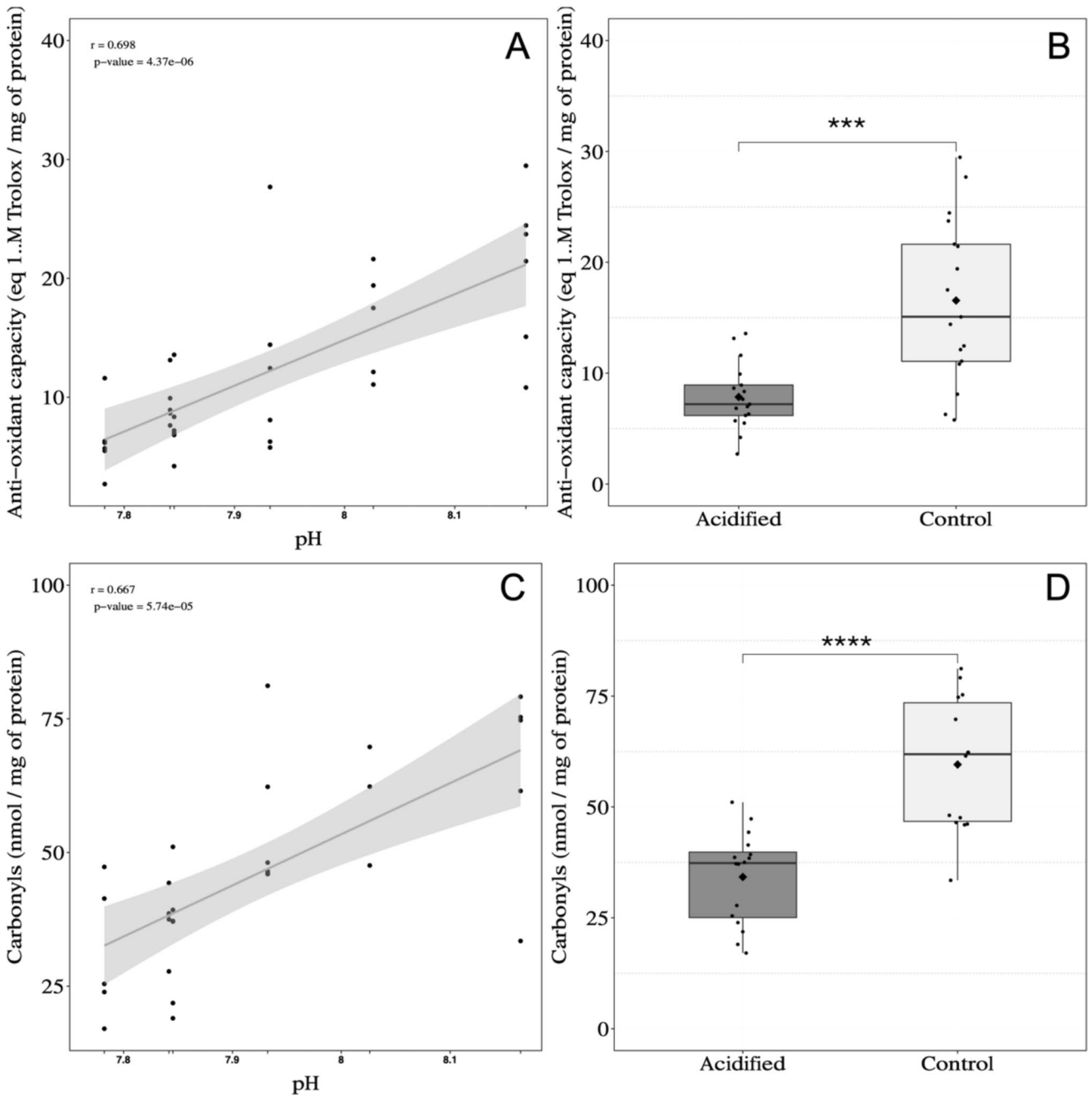

Fig. 5 Redox status of *Porites* cf. *lobata* colonies. Linear regression between antioxidant capacity (**A**) or total carbonyl content (**C**) and pH, with the confidence interval colored in gray. Dots correspond to values measured in each colony. Total antioxidant capacity (**B**) and carbonyl content (**D**) measured at control (light gray; n = 17) and acidified (dark gray; n = 17) sites are represented by boxplot; diamonds represent the mean of each site. Significance: *** ≤ 0.001; **** ≤ 0.0001

(2 mM), which is used by corals for photosynthesis and calcification (Furla et al. 2000b). Here, photosynthetic parameters (Pnet and Fv/Fm) and the average symbiont density did not present significant differences between sites (Figs. 3C, 7A, C). The symbiotic relationship between the cnidarian host and its dinoflagellate partner present complex responses to ocean acidification, as reviewed by Hill and Hoogenboom (2022). Most studies did not observe a significant effect of ocean acidification on photosynthesis rate or its efficiency (e.g., Kroeker et al. 2013a, b; Bedwell-Ivers et al. 2017; Bahr et al. 2018), symbiont lineage, symbiont density or chlorophyll concentration (e.g., Fabricius et al. 2004; Rivest and Hofmann 2014; Bedwell-Ivers et al. 2017). However, some studies have found contrasting results, showing enhanced

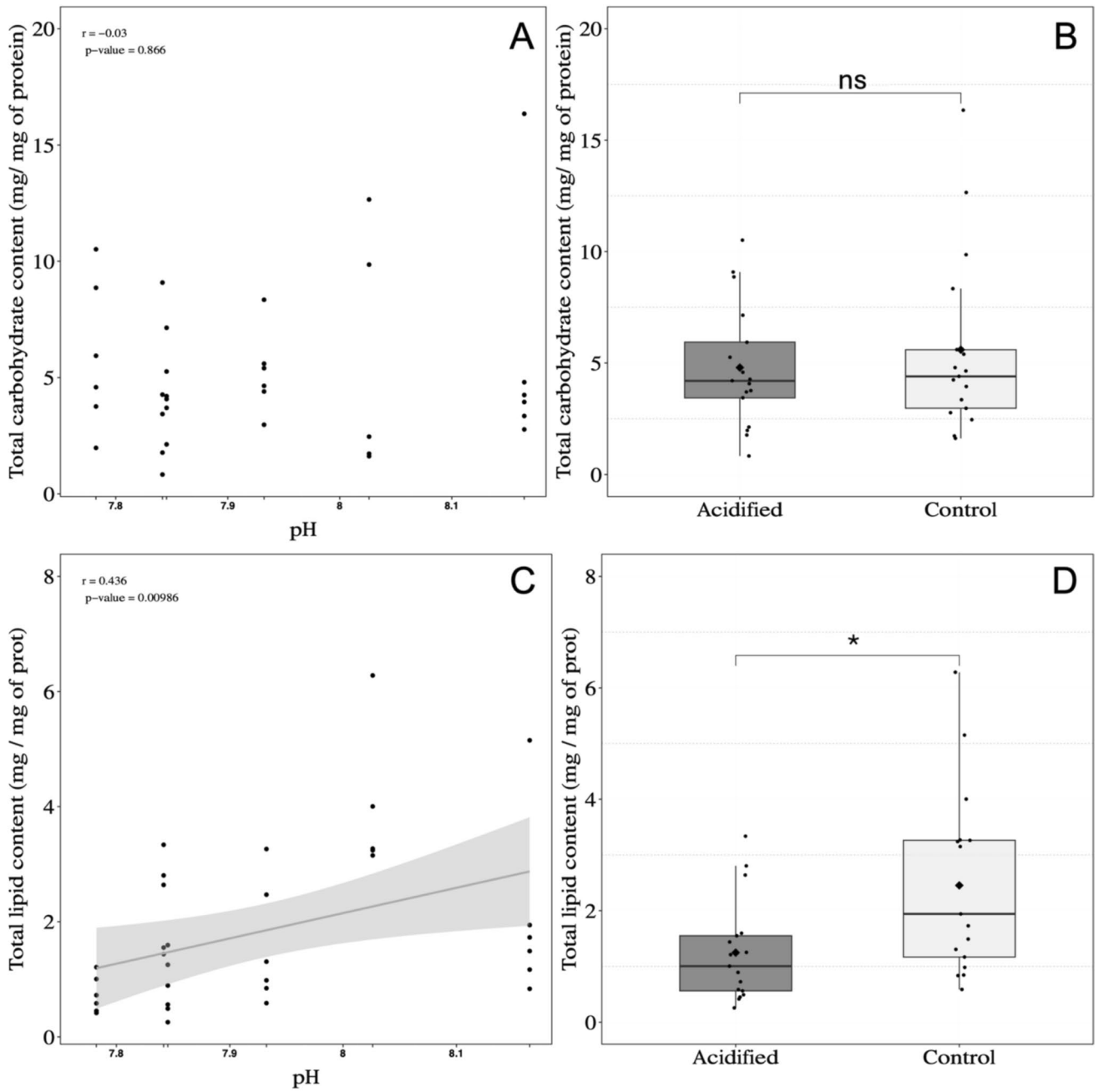

Fig. 6 Energetic content of *Porites* cf. *lobata* colonies. Linear regression between total carbohydrate (**A**) or lipid (**C**) content and pH with the confidence interval colored in gray. Dots correspond to values measured in each colony. Total carbohydrate (**B**) and lipid (**D**) content measured at control (light gray; n = 17) and acidified (dark gray; n = 17) sites are represented by boxplot; diamonds represent the mean of each site. Significance: n.s > 0.05; * ≤ 0.05

photochemistry and translocation of photosynthates to the host (Krueger et al. 2017, 2018; Sun et al. 2024), while others show decreases in productivity and symbiont density (Anthony et al. 2008; Kaniewska et al. 2012). Herrera and coworkers (2021) showed that despite an up-regulation in genes related to photosynthesis in the endosymbionts of *Stylophora pistillata* under long-term low-pH conditions, the efficiency of photosynthesis is decreased. Differences in experimental setup and species-specific responses can explain the contradicting observations, making it difficult to make general assumptions. Nevertheless, our study demonstrated the *Porites* cf. *lobata* colonies in Palau archipelago were able to cope with ocean acidification, suggesting a good robustness on future changing environment. These results are in line with observations of Kurihara and collaborators (2021) who found no differences in the net photosynthesis

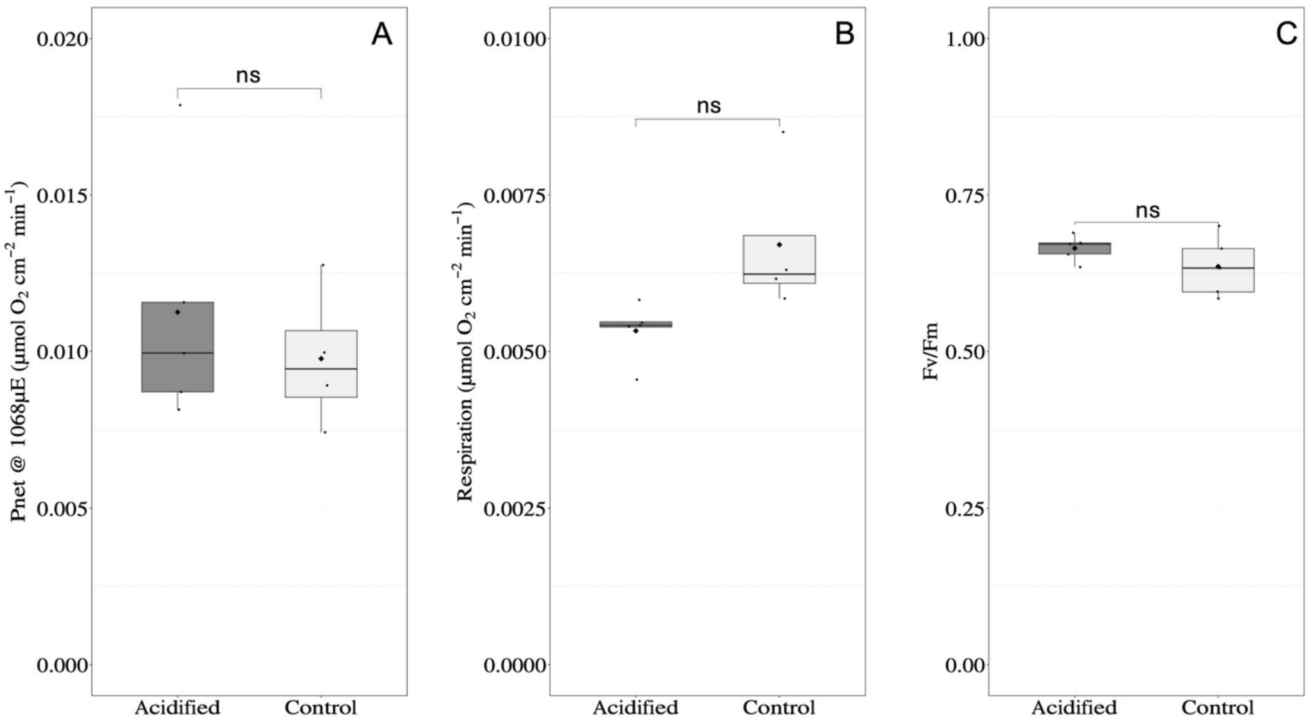

Fig. 7 Photosynthetic parameter of *Porites* cf. *lobata* colonies. Net photosynthesis (**A**), respiration (**B**), and Fv/Fm ratio (**C**) from colonies sampled in control (light gray; n = 5) and acidified (dark gray; n = 5) sites. Dots correspond to values measured in each colony; diamonds represent the mean of each site. Significance: n.s > 0.05

of *Porites cylindrica* in Nikko Bay. The $\delta^{13}C$ signatures of animal tissues serve as a long-term index of carbon assimilation (Muscatine et al. 1989), and are also a useful tool for understanding the trophic status of animals (Bergschneider and Muller-parker 2008; Price et al. 2021). In symbiotic corals, the carbon isotopic compositions reflect the assimilation of different sources of nutrition including heterotrophic prey (such as plankton preys) and the photosymbiont-derived carbon source through the fixation of inorganic carbon by photosynthetic activity (Nahon et al. 2013). The $\delta^{13}C$ values obtained in the present study for animal tissue and symbiont (Fig. 2) were in agreement with previously measured values for symbiotic corals (Reynaud et al. 2002; Fujii et al. 2020). As a result of isotopic fractionation associated with reciprocal exchanges of carbon between hosts and photosymbionts, animal tissues were C-depleted compared to their photosymbiont (Reynaud et al. 2002; Lesser et al. 2022). The carbon isotopic signature of coral tissues suggests a predominantly autotrophic carbon supply at both sites, with less reliance on heterotrophic sources. At the acidified site, autotrophy appears to be even more dominant, as suggested by the greater difference in $\delta^{13}C$ values between coral tissues and plankton.

Studies have shown that carbon isotope discrimination may vary due to cellular physiological responses and environmental factors such as the pH (Roeske and O'Leary 1985; Hinga et al. 1994; Brandenburg et al. 2022). In the acidified sites of the present work, the carbon isotopic signature of the symbionts did not change, whereas the $\delta^{13}C$ values of the animal tissues decreased sharply (Fig. 2). Taking into account that the amount of dissolved CO_2 in the seawater in acidified sites was roughly the double (Table 1), and since dissolved CO_2 typically has a lower $\delta^{13}C$ than HCO_3^- (Mook et al. 1974; Reynaud et al. 2002), we could conclude that the decrease in $\delta^{13}C$ values of the animal tissues could reflect a change in inorganic carbon source for photosynthesis. Indeed, an increase in the uptake of dissolved CO_2, which depleted the $\delta^{13}C$, is then responsible for animal tissue carbon isotope discrimination, supporting a switch of CO_2-user coral. These findings are consistent with previous results showing that in acidified environments, where dissolved CO_2 concentrations are higher, corals tend to uptake more ^{12}C rich-CO_2 for photosynthesis (Nahon et al. 2013). This change in the source of inorganic carbon for photosynthesis is also brought by the carbonic anhydrase activity reduction (Fig. 4) in acidified sites.

In the symbiotic state, the coral host acts as a phototrophic organism, converting bicarbonate into carbon dioxide through the action of proton pump and carbonic anhydrase enzymes (Weis et al. 1989; Furla et al. 2000a, b; 2005; Bertucci et al. 2010). However, as pCO_2 is considerably increased under ocean acidification, CO_2 becomes more

available for biological usage. In our study, carbonic anhydrase activity positively correlates with pH (Fig. 4). This decrease in carbonic anhydrase activity at lower pH has also been documented in other symbiotic non-calcifying and calcifying cnidarians. Ventura et al. (2016) observed a 30% decrease in total animal carbonic anhydrase activity of the temperate sea anemone *Anemonia viridis* in acidified sites of Vulcano Island (Italy). Other studies have also reported downregulation of carbonic anhydrase gene expression in *Acropora millepora* juveniles (Moya et al. 2012) and *Stylophora pistillata* (Zoccola et al. 2016). This decrease has been suggested as a mechanism to preserve energy, favoring the passive diffusion of CO_2 that does not require energy investment from the host (Ventura et al. 2016). Indeed, the lower activity in low-pH conditions can be linked to a change in inorganic carbon source from HCO_3^- to CO_2 for photosynthesis (Horwitz et al. 2015).

The reduction in $\delta^{13}C$ values of animal tissues and symbionts, as well as carbonic anhydrases activities reduced strongly support that under low-pH conditions, the modulation of inorganic carbon uptake processes in *Porites* cf. *lobata* ensures host-symbiont trophic relationships. By becoming a higher CO_2-user compared to HCO_3^-, corals might have an economy in the holobiont's energy budget, saving energy for other vital processes like calcification (Beardall and Giordano 2002).

Calcification rate is preserved in low-pH conditions

Corals build their skeleton by actively removing protons from the calcifying fluid through a Ca^{2+}-ATPase pump in the calcifying fluid (Al-Horani et al. 2003; Cohen and McConnaughey 2003; Allemand et al. 2004; Zoccola et al. 2004; Venn et al. 2011, 2022). This exchange of ions favors the formation of CO_3^{2-}, which elevates the aragonite saturation state to facilitate calcification. Without the proper animal regulation of the calcifying fluid, the calcification rate is expected to decrease under low-pH conditions (Gattuso et al. 1999; Cohen and McConnaughey 2003; Erez et al. 2011; Holcomb et al. 2014; Comeau et al. 2022). Here, the analysis of the *Porites* cf. *lobata* skeleton cores showed that the calcification rate is maintained under low-pH conditions. These results indicate that *Porites* cf. *lobata* can maintain the pH homeostasis of the calcifying fluid. It is consistent with previous research on massive *Porites* species in which the chemistry of the calcifying fluid was not affected by external seawater chemistry (Comeau et al. 2019; Canesi et al. 2024), therefore sustaining calcification (Fabricius et al. 2011; Edmunds et al. 2012; Comeau et al. 2014a, b). Similar results were observed in *Porites*' colonies from Papua New Guinea, living at CO_2-seeps, where growth rates were maintained under low-pH conditions (Fabricius et al. 2011; Wall et al. 2016), showing the high buffering capacity of this genus to lower pH. In addition, previous studies in the Palau archipelago have shown hints of high resistance of these Palauan corals. Barkley et al. (2017) showed that *Porites* colonies maintained calcification rates over a Ωar range from 3.0 to 1.5 regardless of site origin and without additional environmental factors, such as nutrients, light, or temperature. An increased Ca^{2+}-ATPase pump activity can explain this high tolerance (Al-Horani et al. 2003). Indeed, Canesi et al. (2024) found that from 1972 to 2015, *Porites* colonies drilled in control and more acidified sites presented comparable carbonate chemistry in their calcifying fluid, translating to higher energetic effort for the coral to sustain calcification (Canesi et al. 2024).

Nevertheless, previous research has demonstrated a limit to the buffering capacity of *Porites* corals. The formation of the coral skeleton is dependent on their soft tissue arrangement (Tambutté et al. 2007); therefore, changes in the calicodermis induce modification in organic matrix microstructure (Tambutté et al. 2015; Coronado et al. 2019). Our results are consistent with the literature as skeleton density decreases in acidified sites compared to controls (Mollica et al. 2018; D'Olivo et al. 2019; Guo et al. 2020) while linear extension increases (Canesi et al. 2024) (Table 2). However, these results should be interpreted cautiously due to the limited number of cored colonies—only one per site. Future studies should increase the number of cores sampled to strengthen and validate these findings. Besides, ocean acidification can induce calcification's "structural" differences (Marubini et al. 2003; Cohen et al. 2009; Tambutté et al. 2015) which should also be investigated. Factors such as the ratio of centers of calcification (COC) to aragonite fibers, the composition and size of COCs (Cuif and Dauphin 1998; Cohen and Holcomb 2009), and the quantity and composition of the microborer community (Tribollet et al. 2009, 2019; DeCarlo et al. 2015) are known to be influenced by environmental conditions, including seawater acidification.

Under low-pH conditions, the energy demand for increased Ca^{2+}-ATPase pump activity can be met through the energy economy by more efficient utilization of CO_2. This energy can, therefore, be reallocated toward calcification. Overall, these results suggest that the energy budget in *Porites* cf. *lobata* living in an acidified site is sufficient to sustain calcification rates, although the skeleton structure is modified.

Changes in metabolic pathways

Maintaining calcification in an acidifying ocean requires more energy input (McCulloch et al. 2012; Spalding et al. 2017). One potential strategy to conserve energy is to utilize available CO_2 directly for the photosynthetic needs of the symbionts, rather than relying on the conversion of bicarbonate. This energy-saving mechanism could then redirect

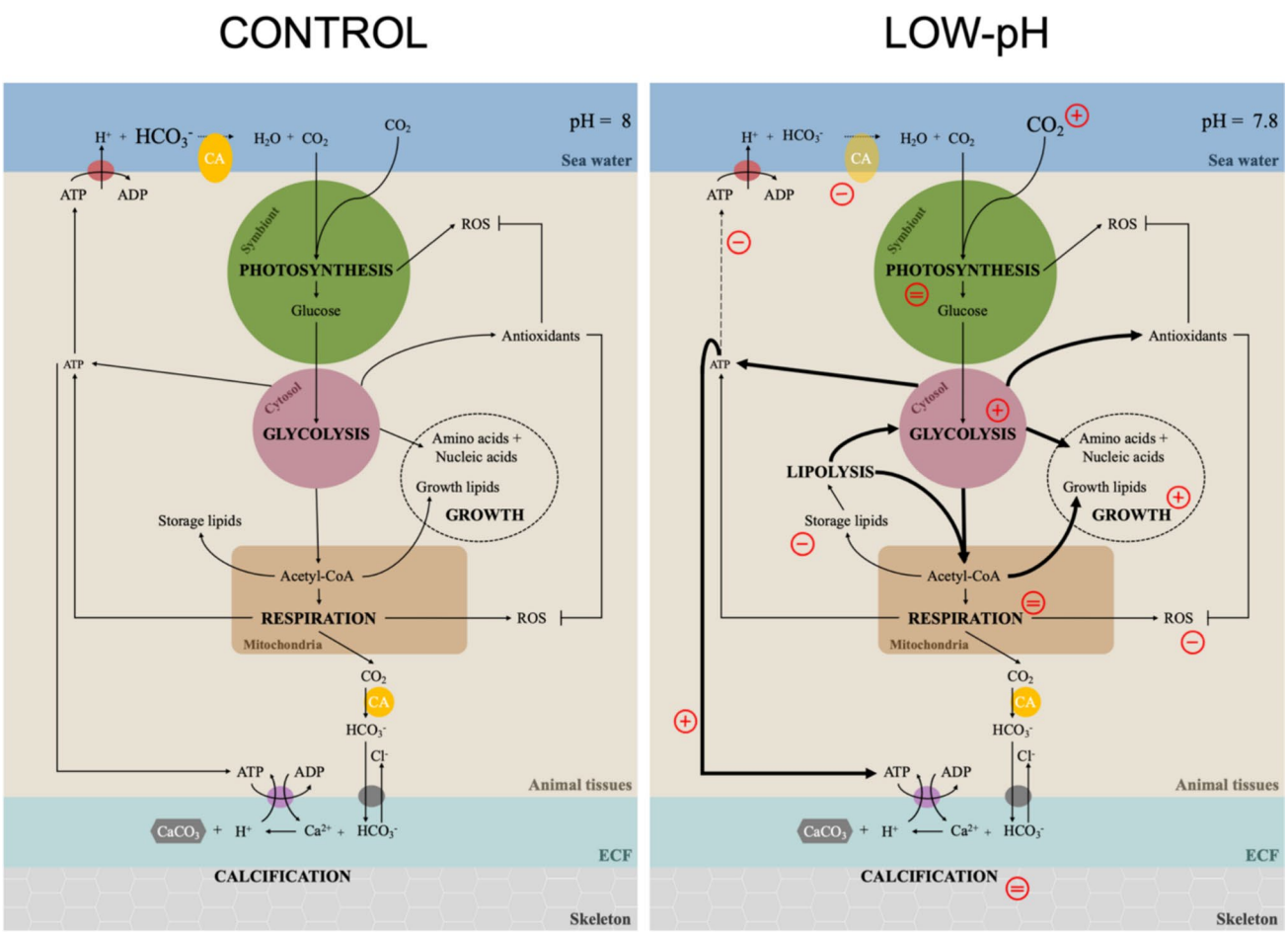

Fig. 8 Metabolic shifts in *Porites* cf. *lobata* coral from the Palau archipelago under low-pH conditions. (**A**) Under control conditions, the coral host invests energy to increase pCO_2 in the epidermal boundary layer using HCO_3^- as an inorganic carbon source for photosynthesis by the synergistic action of H^+-ATPase pumps and carbonic anhydrases. CO_2 diffuses through the tissues and reaches the photosynthetic endosymbionts, where glucose is produced and partially transferred to the host to support its heterotrophic metabolism. Within host cells, glucose is used (i) for energy demand via glycolysis and mitochondrial respiration (generating ATP for HCO_3^- uptake for photosynthesis and to support calcification in the extracellular calcifying fluid (ECF) and (ii) for biomass growth through conversion into amino acids, nucleic acids, and structural lipids. The excess organic carbon is then stored in the host cells as storage lipids. Electron transfer in photosynthesis and mitochondrial respiration processes are sources of ROS that are constantly neutralized by antioxidant defenses. (**B**) Under low-pH conditions, pCO_2 is increased by atmospheric CO_2 dissolution, favoring passive diffusion of CO_2 for photosynthetic needs. While maintaining an unchanged photosynthetic rate, the increased CO_2 source of inorganic carbon reduces the ATP requirement for HCO_3^- uptake, allowing ATP to be reallocated to support calcification. In fact, under acidic conditions, the coral has to allocate more energy to achieve a favorable pH for calcification in its extracellular calcifying fluid through the action of Ca^{2+}-ATPase. In addition, to meet this increased energy demand, lipid reserves are mobilized through lipolysis, producing glycerol and fatty acids that fuel respiration via β-oxidation. Increased fatty acids content also increases the building blocks of cell membranes, stimulating cell proliferation and ultimately animal biomass. At the same time, the redox status decreases due to this metabolic shift, where lipolysis and glycolysis regulation play a critical role

resources toward calcification processes. Another strategy involves optimizing energy efficiency by enhancing the functionality of cellular metabolism (Dellisanti et al. 2022). In this study, we observed a decrease in lipid content along the pH gradient (Fig. 6 C, D), while total carbohydrates were similar between sites (Fig. 6A, B). The decrease of lipids, a long-term energetic reserve, may reflect a higher mobilization of the compounds for cellular metabolism, as described for *Acropora millepora* (Kaniewska et al. 2012). Under high pCO_2 conditions, *A. millepora* showed an up-regulation of triglyceride lipase and acyl-CoA dehydrogenase, enzymes involved in lipolysis. Along with fatty acid oxidation, increased respiration rates and oxidative stress would be expected due to the increase in ROS as a by-product of aerobic metabolism (Vidal-Dupiol et al. 2013; Davies et al. 2016; Abou-Rjeileh and Contreras 2021; Agostini et al. 2021). Surprisingly, in the acidified site, the respiration rates of *Porites* cf. *lobata* colonies remained unaffected, similar to

the observations made by Kurihara and collaborators (2021) in *Porites cylindrica*. However, the redox state of our colonies was reduced, accompanied by lower total antioxidant defenses and protein damage (Fig. 5). To interpret the cellular traits observed in *Porites* cf. *lobata* at the acidified site, we propose an increase in lipid mobilization to promote less efficient metabolic pathways such as glycolysis and its derivatives. Glycolysis is the metabolic pathway that converts glucose into pyruvate or lactate in the cytoplasm, generating ATP and NADH in the absence of oxygen to produce lactate as the end product and keep glycolysis and ATP generation ongoing (Robergs et al. 2004; Chaudhry and Varacallo 2023). This later process has been described in cnidarians under hypoxic conditions (e.g., Sassaman and Mangum 1973; Murphy and Richmond 2016; Linsmayer et al. 2020). Vidal-Dupiol et al. (2013) observed an up-regulation of glycolysis gene expression in *Pocillopora damicornis* after 3 weeks of exposure to low pH conditions, supporting the possibility that ocean acidification can trigger switches in metabolic pathways (Vidal-Dupiol et al. 2013). However, the capacity to enhance this or alternative metabolic pathways under ocean acidification has been poorly investigated. We propose that glycolysis is increased under low-pH conditions to facilitate rapid ATP production in a Warburg-like effect. The Warburg effect was first described in cancer cells, where the cell undergoes glycolysis and lactate production even in the presence of oxygen to support processes such as cell proliferation (Warburg and Minami 1923; Warburg 1925; Liberti and Locasale 2016). The so-called aerobic glycolysis is not limited to cancer cells but also occurs in exercising muscle cells (Lee 2021), which may be similar to what is observed under low-pH conditions. Intermediate molecules from glycolysis and lactic fermentation can be diverted to proteins, lipids, or nucleotide biosynthesis (Mullarky and Cantley 2015; Liberti and Locasale 2016; DeBerardinis and Chandel 2020), allowing higher cell proliferation and increasing biomass. The coral tissue may act as a protective barrier for the site of calcification (Jokiel 2011; Rodolfo-Metalpa et al. 2011), particularly in *Porites*, as their tissue is known to be thick (Edmunds 2011). The increased animal biomass might mitigate the effects of decreasing pH on calcification (Ries 2011; McCulloch et al. 2012). The observed rise in animal biomass at the acidified sites compared to control sites could potentially be explained by enhanced glycolysis. As a flexible and pivotal pathway in cellular metabolism, glycolysis can also be redirected to fight oxidative stress, which may account for the observed reduction in redox state (Mullarky et al. 2015). These results suggest that *Porites* cf. *lobata* colonies undergo metabolic shifts that enable them to adapt to low-pH conditions, as illustrated in Fig. 8.

Conclusions

Our analysis revealed the resilience of *Porites* cf. *lobata* corals in the Palau archipelago under lower pH and higher pCO_2 levels. Acidified conditions enhance CO_2 diffusion through coral tissues, reducing ATPase and carbonic anhydrase activity. Despite these changes, photosynthesis and carbohydrate levels remain stable, allowing energy redirection toward calcification. Metabolic rates stay constant, but oxidative stress and lipid reserves decline, indicating potential alterations in metabolic pathways akin to the Warburg effect. This suggests that glycolysis may serve as a coping mechanism for these corals. Despite their adaptability, reduced lipid content and lower skeleton density could weaken resistance to stressors like heat waves, storms, and infections, risking energy depletion and ultimately leading to coral death. Our findings highlight the evolutionary flexibility of *Porites* cf. *lobata* corals, contributing to the hypothesis of "winning" corals under ocean acidification. Future research should explore these metabolic mechanisms in natural populations across seasons, filling knowledge gaps in coral metabolism that may vary by species, location, or the degree of acidification.

Acknowledgements Special thanks to the Tara Ocean Foundation, the R/V Tara crew and the Tara Pacific Expedition Participants (https://doi.org/10.5281/zenodo.3777760). We are keen to thank the commitment of the following institutions for their financial and scientific support that made this unique Tara Pacific Expedition possible: CNRS, PSL, CSM, EPHE, Genoscope, CEA, Inserm, Université Côte d'Azur, ANR, agnès b., UNESCO-IOC, the Veolia Foundation, the Prince Albert II de Monaco Foundation, Région Bretagne, Billerudkorsnas, AmerisourceBergen Company, Lorient Agglomération, Oceans by Disney, L'Oréal, Biotherm, France Collectivités, Fonds Français pour l'Environnement Mondial (FFEM), Etienne Bourgois, and the Tara Ocean Foundation teams. Tara Pacific would not exist without the continuous support of the participating institutes. The authors also particularly thank Serge Planes, Denis Allemand, and the Tara Pacific consortium. We are keen to thank the local people and authorities who made this study possible. Specifically, we thank the Ministry of Natural Resources, Environment & Tourism of Republic of Palau. For the experimental and analytic support, we thank Cécile Rottier for preparing the samples prior to the carbon isotope analysis and Thamilla Zamoum and Alexis Pey for preparing the PALAU expedition. We also thank Josephine Michelot for the animal biomass and symbiont density analysis. We are grateful to referees and the topic editor for their constructive comments.

Author contributions K.P: Data curation, Investigation, Formal analysis, Methodology, Writing—original draft M.T: Data curation, review & editing S.R: Data curation, Investigation, Formal analysis, Methodology, Validation, Writing—original draft, review & editing M.C: Data curation, Investigation, Formal analysis, Methodology, Validation, Writing—original draft, review & editing Eric Béraud: Data curation, Investigation, Formal analysis, Methodology, Validation, Writing—review & editing E.D: Data curation, Investigation, Writing—review & editing Didier Zoccola: Investigation, Writing—review & editing E.G: Investigation, Writing—review & editing S.R:

Conceptualization, Data curation, Investigation, Formal analysis, Funding acquisition, Investigation, Methodology, Supervision, Writing—original draft, review & editing P.F: Conceptualization, Data curation, Investigation, Formal analysis, Funding acquisition, Methodology, Supervision, Writing—original draft, review & editing.

Funding The work was supported by the ANR CORALGENE (ANR-17-CE02-0020), by the ANR CORALFORCE (ANR-22-CE20-0007) and by the doctoral fellowship from the French Ministère de l'Enseignement Supérieur et de la Recherche to K.P. This collaborative study was also partly supported by the Government of the Principality of Monaco.

Data Availability Raw data has been deposited in Zenodo and is available via the link shared in the material and methods section of the manuscript. The data will be released public once the article is published.

Declarations

Competing Interests The authors declare no competing interests.

Referencesss

Abou-Rjeileh U, Contreras GA (2021) Redox regulation of lipid mobilization in adipose tissues. Antioxidants 10:1090. https://doi.org/10.3390/antiox10071090

Agostini S, Houlbrèque F, Biscéré T, Harvey BP, Heitzman JM, Takimoto R, Yamazaki W, Milazzo M, Rodolfo-Metalpa R (2021) Greater mitochondrial energy production provides resistance to ocean acidification in "Winning" hermatypic corals. Front Mar Sci 7:600836. https://doi.org/10.3389/fmars.2020.600836

Alaguarda D, Brajard J, Coulibaly G, Canesi M, Douville E, Le Cornec F, Lelabousse C, Tribollet A (2022) 54 years of microboring community history explored by machine learning in a massive coral from Mayotte (Indian Ocean). Front Mar Sci 9:899398. https://doi.org/10.3389/fmars.2022.899398

Al-Horani FA, Al-Moghrabi SM, de Beer D (2003) The mechanism of calcification and its relation to photosynthesis and respiration in the scleractinian coral Galaxea fascicularis. Mar Biol 142:419–426. https://doi.org/10.1007/s00227-002-0981-8

Allemand D, Ferrier-Pagès C, Furla P, Houlbrèque F, Puverel S, Reynaud S, Tambutté É, Tambutté S, Zoccola D (2004) Biomineralisation in reef-building corals: from molecular mechanisms to environmental control. C R Palevol 3:453–467. https://doi.org/10.1016/J.CRPV.2004.07.011

Andersson AJ, Mackenzie FT, Gattuso J-P (2011) Effects of Ocean Acidification on Benthic Processes, Organisms, and Ecosystems, in: Ocean Acidification. Oxford University Press. https://doi.org/10.1093/oso/9780199591091.003.0012

Anthony KRN, Kline DI, Diaz-Pulido G, Dove S, Hoegh-Guldberg O (2008) Ocean acidification causes bleaching and productivity loss in coral reef builders. Proc Natl Acad Sci 105:17442–17446. https://doi.org/10.1073/pnas.0804478105

Bahr KD, Rodgers KS, Jokiel PL (2018) Ocean warming drives decline in coral metabolism while acidification highlights species-specific responses. Mar Biol Res 14:924–935. https://doi.org/10.1080/17451000.2018.1551616

Barkley HC, Cohen AL, McCorkle DC, Golbuu Y (2017) Mechanisms and thresholds for pH tolerance in Palau corals. J Exp Mar Biol Ecol 489:7–14. https://doi.org/10.1016/j.jembe.2017.01.003

Beardall J, Giordano M (2002) Ecological implications of microalgal and cyanobacterial CO_2 concentrating mechanisms, and their regulation. Funct Plant Biol 29:335. https://doi.org/10.1071/PP01195

Bedwell-Ivers HE, Koch MS, Peach KE, Joles L, Dutra E, Manfrino C (2017) The role of in hospite zooxanthellae photophysiology and reef chemistry on elevated pCO_2 effects in two branching Caribbean corals: Acropora cervicornis and Porites divaricata. ICES J Mar Sci 74:1103–1112. https://doi.org/10.1093/icesjms/fsw026

Bergschneider H, Muller-parker G (2008) Nutritional role of two algal symbionts in the temperate sea anemone *Anthopleura elegantissima* brandt. Biol Bull 215:73–88. https://doi.org/10.2307/25470685

Bertucci A, Tambutté É, Tambutté S, Allemand D, Zoccola D (2010) Symbiosis-dependent gene expression in coral–dinoflagellate association: cloning and characterization of a P-type H^+ -ATPase gene. Proceedings of the Royal Society B: Biological Sciences 277:87–95. https://doi.org/10.1098/rspb.2009.1266

Biscéré T, Zampighi M, Lorrain A, Jurriaans S, Foggo A, Houlbrèque F, Rodolfo-Metalpa R (2019) High pCO_2 promotes coral primary production. Biol Lett 15:20180777. https://doi.org/10.1098/rsbl.2018.0777

Bradford M (1976) A rapid and sensitive method for the quantitation of microgram quantities of protein utilizing the principle of protein-dye binding. Anal Biochem 72:248–254. https://doi.org/10.1006/abio.1976.9999

Brandenburg KM, Rost B, Van de Waal DB, Hoins M, Sluijs A (2022) Physiological control on carbon isotope fractionation in marine phytoplankton. Biogeosciences 19:3305–3315. https://doi.org/10.5194/bg-19-3305-2022

Brownlee C (2009) pH regulation in symbiotic anemones and corals: a delicate balancing act. Proc Natl Acad Sci 106:16541–16542. https://doi.org/10.1073/pnas.0909140106

Buss H, Timothy P, Chan Karl B, Sluis Neil M, Domigan Christine C, Winterbourn (1997) Protein Carbonyl Measurement by a Sensitive ELISA Method Free Radical Biology and Medicine 23(3):361-366 https://doi.org/10.1016/S0891-5849(97)00104-4

Bythell JC, Brown BE, Kirkwood TBL (2018) Do reef corals age? Biol Rev 93:1192–1202. https://doi.org/10.1111/brv.12391

Canesi M, Douville É, Bordier L, Dapoigny A, Coulibaly GE, Montagna P, Béraud É, Allemand D, Planes S, Furla P, Gilson E, Roberty S, Zoccola D, Reynaud S (2024) Porites' coral calcifying fluid chemistry regulation under normal- and low-pH seawater conditions in Palau Archipelago: Impacts on growth properties. Sci Total Environ 911:168552. https://doi.org/10.1016/j.scitotenv.2023.168552

Chaudhry R, Varacallo M (2023) Biochemistry. StatPearls Publishing, Treasure Island (FL), Glycolysis

Cheng Y, Zheng Y, VanderGheynst JS (2011) Rapid quantitative analysis of lipids using a colorimetric method in a microplate format. Lipids 46:95–103. https://doi.org/10.1007/s11745-010-3494-0

Clayton TD, Byrne RH (1993) Spectrophotometric seawater pH measurements: total hydrogen ion concentration scale calibration of m-cresol purple and at-sea results. Deep-Sea Res I Oceanogr Res Pap 40:2115–2129

Cohen A, Holcomb M (2009) Why corals care about ocean acidification: uncovering the mechanism. Oceanography 22:118–127. https://doi.org/10.5670/oceanog.2009.102

Cohen AL, McConnaughey TA (2003) Geochemical perspectives on coral mineralization. Rev Mineral Geochem 54:151–187. https://doi.org/10.2113/0540151

Cohen AL, McCorkle DC, De Putron S, Gaetani GA, Rose KA (2009) Morphological and compositional changes in the skeletons of new coral recruits reared in acidified seawater: insights into the biomineralization response to ocean acidification. Geochem, Geophys, Geosyst. https://doi.org/10.1029/2009GC002411

Comeau S, Carpenter RC, Nojiri Y, Putnam HM, Sakai K, Edmunds PJ (2014a) Pacific-wide contrast highlights resistance of reef calcifiers to ocean acidification. Proceedings of the Royal Society b: Biological Sciences 281:20141339. https://doi.org/10.1098/rspb.2014.1339

Comeau S, Edmunds PJ, Spindel NB, Carpenter RC (2014b) Fast coral reef calcifiers are more sensitive to ocean acidification in short-term laboratory incubations. Limnol Oceanogr 59:1081–1091. https://doi.org/10.4319/lo.2014.59.3.1081

Comeau S, Cornwall CE, DeCarlo TM, Doo SS, Carpenter RC, McCulloch MT (2019) Resistance to ocean acidification in coral reef taxa is not gained by acclimatization. Nat Clim Chang 9:477–483. https://doi.org/10.1038/s41558-019-0486-9

Comeau S, Cornwall CE, Shlesinger T, Hoogenboom M, Mana R, McCulloch MT, Rodolfo-Metalpa R (2022) pH variability at volcanic CO_2 seeps regulates coral calcifying fluid chemistry. Glob Chang Biol 28:2751–2763. https://doi.org/10.1111/gcb.16093

Coronado I, Fine M, Bosellini FR, Stolarski J (2019) Impact of ocean acidification on crystallographic vital effect of the coral skeleton. Nat Commun 10:2896. https://doi.org/10.1038/s41467-019-10833-6

Coward G, Lawrence A, Ripley N, Brown V, Sudek M, Brown E, Moffitt I, Fuiava B, Vargas-Ángel B (2020) A new record for a massive Porites colony at Ta'u Island. American Samoa Sci Rep 10:21359. https://doi.org/10.1038/s41598-020-77776-7

Cuif J-P, Dauphin Y (1998) Microstructural and physico-chemical characterization of 'centers of calcification' in septa of some Recent scleractinian corals. Palaontol Z 72:257–269. https://doi.org/10.1007/BF02988357

D'Olivo JP, Ellwood G, DeCarlo TM, McCulloch MT (2019) Deconvolving the long-term impacts of ocean acidification and warming on coral biomineralisation. Earth Planet Sci Lett 526:115785. https://doi.org/10.1016/J.EPSL.2019.115785

Davies PS (1991) Effect of daylight variations on the energy budgets of shallow-water corals. Mar Biol 108:137–144. https://doi.org/10.1007/BF01313481

Davies SW, Marchetti A, Ries JB, Castillo KD (2016) Thermal and pCO_2 stress elicit divergent transcriptomic responses in a resilient coral. Front Mar Sci 3:112. https://doi.org/10.3389/fmars.2016.00112

Davies SW, Ries JB, Marchetti A, Castillo KD (2018) Symbiodinium functional diversity in the coral siderastrea siderea is influenced by thermal stress and reef environment, but not ocean acidification. Front Mar Sci 5:150. https://doi.org/10.3389/fmars.2018.00150

DeBerardinis RJ, Chandel NS (2020) We need to talk about the Warburg effect. Nat Metab 2:127–129. https://doi.org/10.1038/s42255-020-0172-2

DeCarlo TM, Cohen AL, Barkley HC, Cobban Q, Young C, Shamberger KE, Brainard RE, Golbuu Y (2015) Coral macrobioerosion is accelerated by ocean acidification and nutrients. Geology 43:7–10. https://doi.org/10.1130/G36147.1

DeCarlo TM, D'Olivo JP, Foster T, Holcomb M, Becker T, McCulloch MT (2017) Coral calcifying fluid aragonite saturation states derived from Raman spectroscopy. Biogeosciences 14:5253–5269. https://doi.org/10.5194/bg-14-5253-2017

Dellisanti W, Seveso D, Kar-Hei Fang J (2022) Nutrition of Corals and Their Trophic Plasticity under Future Environmental Conditions. In: Corals-Habitat Formers in the Anthropocene. IntechOpen. https://doi.org/10.5772/intechopen.104612

Dickson AG (1990) Thermodynamics of the dissociation of boric acid in synthetic seawater from 273.15 to 318.15 K. Deep sea research part A. Oceanogr Res Pap 37:755–766. https://doi.org/10.1016/0198-0149(90)90004-F

Dickson AG, Millero FJ (1987) A comparison of the equilibrium constants for the dissociation of carbonic acid in seawater media. Deep sea research part A. Oceanogr Res Pap 34:1733–1743. https://doi.org/10.1016/0198-0149(87)90021-5

Dickson AG, Sabine CL, Christian, Robert J (2007) Guide to best practices for ocean CO_2 measurements. North Pacific Marine Science Organization

Edmunds PJ (2011) Zooplanktivory ameliorates the effects of ocean acidification on the reef coral Porites spp. Limnol Oceanogr 56:2402–2410. https://doi.org/10.4319/lo.2011.56.6.2402

Edmunds PJ, Brown D, Moriarty V (2012) Interactive effects of ocean acidification and temperature on two scleractinian corals from Moorea, French Polynesia. Glob Chang Biol 18:2173–2183. https://doi.org/10.1111/j.1365-2486.2012.02695.x

Erez J, Reynaud S, Silverman J, Schneider K, Allemand D (2011) Coral calcification under ocean acidification and global change. In: Coral Reefs: An Ecosystem in Transition. Springer Netherlands, pp. 151–176. https://doi.org/10.1007/978-94-007-0114-4_10

Fabricius KE, Mieog JC, Colin PL, Idip D, Van Oppen MJH (2004) Identity and diversity of coral endosymbionts (zooxanthellae) from three Palauan reefs with contrasting bleaching, temperature and shading histories. Mol Ecol 13:2445–2458. https://doi.org/10.1111/j.1365-294X.2004.02230.x

Fabricius KE, Langdon C, Uthicke S, Humphrey C, Noonan S, De'ath G, Okazaki R, Muehllehner N, Glas MS, Lough JM (2011) Losers and winners in coral reefs acclimatized to elevated carbon dioxide concentrations. Nat Clim Chang 1:165–169. https://doi.org/10.1038/nclimate1122

Flora CJ, Ely PS (2003) Surface growth rings of Porites lutea microatolls accurately track their annual growth. Northwest Sci 77:237–245

Forsman ZH, Ritson-Williams R, Tisthammer KH, Knapp ISS, Toonen RJ (2020) Host-symbiont coevolution, cryptic structure, and bleaching susceptibility, in a coral species complex (Scleractinia; Poritidae). Sci Rep 10:16995. https://doi.org/10.1038/s41598-020-73501-6

Fujii T, Tanaka Y, Maki K, Saotome N, Morimoto N, Watanabe A, Miyajima T (2020) Organic carbon and nitrogen isoscapes of reef corals and algal symbionts: relative influences of environmental gradients and heterotrophy. Microorganisms 8:1–26. https://doi.org/10.3390/microorganisms8081221

Furla P, Allemand D, Orsenigo M-N (2000a) Involvement of H^+-ATPase and carbonic anhydrase in inorganic carbon uptake for endosymbiont photosynthesis. Am J Physiol-Regul, Integr Comp Physiol 278:R870–R881. https://doi.org/10.1152/ajpregu.2000.278.4.R870

Furla P, Galgani I, Durand I, Allemand D (2000b) Sources and mechanisms of inorganic carbon transport for coral calcification and photosynthesis. J Exp Biol 203(22):3445–3457

Furla P, Allemand D, Shick JM, Ferrier-Pagès C, Richier S, Plantivaux A, Merle PL, Tambutté S (2005) The symbiotic anthozoan: a physiological chimera between alga and animal. Integr Comp Biol 45:595–604. https://doi.org/10.1093/icb/45.4.595

Gattuso J-P, Allemand D, Frankignoulle M (1999) Photosynthesis and calcification at cellular, organismal and community levels in coral reefs: a review on interactions and control by carbonate chemistry. Am Zool 39:160–183. https://doi.org/10.1093/icb/39.1.160

Gattuso J-P, Hansson L (2011) Acidification: background and history. In: Ocean acidification. Oxford University Press. https://doi.org/10.1093/oso/9780199591091.003.0006

Golbuu Y, Gouezo M, Kurihara H, Rehm L, Wolanski E (2016) Long-term isolation and local adaptation in Palau's Nikko Bay help corals thrive in acidic waters. Coral Reefs 35:909–918. https://doi.org/10.1007/s00338-016-1457-5

González-Delgado S, Hernández JC (2018) The Importance of Natural Acidified Systems in the Study of Ocean Acidification: What

Have We Learned? pp. 57–99. https://doi.org/10.1016/bs.amb.2018.08.001

Gruber N, Clement D, Carter BR, Feely RA, van Heuven S, Hoppema M, Ishii M, Key RM, Kozyr A, Lauvset SK, Lo Monaco C, Mathis JT, Murata A, Olsen A, Perez FF, Sabine CL, Tanhua T, Wanninkhof R (2019) The oceanic sink for anthropogenic CO_2 from 1994 to 2007. Science (1979) 363:1193–1199. https://doi.org/10.1126/science.aau5153

Guo W, Bokade R, Cohen AL, Mollica NR, Leung M, Brainard RE (2020) Ocean acidification has impacted coral growth on the Great Barrier Reef. Geophys Res Lett 47:e2019GL086761. https://doi.org/10.1029/2019GL086761

Heinrich Friedrich, Link Beschreibung der Naturalien-Sammlung der Universität zu Rostock Gedruckt bey Adlers Erben Rostock

Highsmith RC (1979) Coral growth rates and environmental control of density banding. J Exp Mar Biol Ecol 37:105–125. https://doi.org/10.1016/0022-0981(79)90089-3

Hill TS, Hoogenboom MO (2022) The indirect effects of ocean acidification on corals and coral communities. Coral Reefs. https://doi.org/10.1007/s00338-022-02286-z

Hinga KR, Arthur MA, Pilson MEQ, Whitaker D (1994) Carbon isotope fractionation by marine phytoplankton in culture: the effects of CO_2 concentration, *p* H, temperature, and species. Global Biogeochem Cycles 8:91–102. https://doi.org/10.1029/93GB03393

Hoegh-Guldberg O (1988) A method for determining the surface area of corals. Coral Reefs 7:113–116. https://doi.org/10.1007/BF00300970

Holcomb M, Venn AA, Tambutté E, Tambutté S, Allemand D, Trotter J, McCulloch M (2014) Coral calcifying fluid pH dictates response to ocean acidification. Sci Rep 4:5207. https://doi.org/10.1038/srep05207

Horwitz R, Borell EM, Yam R, Shemesh A, Fine M (2015) Natural high pCO2 increases autotrophy in Anemonia viridis (Anthozoa) as revealed from stable isotope (C, N) analysis. Sci Rep 5:8779. https://doi.org/10.1038/srep08779

Inoue M, Nakamura T, Tanaka Y, Suzuki A, Yokoyama Y, Kawahata H, Sakai K, Gussone N (2018) A simple role of coral-algal symbiosis in coral calcification based on multiple geochemical tracers. Geochim Cosmochim Acta 235:76–88. https://doi.org/10.1016/j.gca.2018.05.016

IPCC (2018) Global Warming of 1.5 °C. An IPCC Special Report on the impacts of global warming of 1.5 °C above pre-industrial levels and related global greenhouse gas emission pathways, in the context of strengthening the global response to the threat of climate change, sustainable development, and efforts to eradicate poverty [Masson-Delmotte V, Zhai P, Pörtner H-O, Roberts D, Skea J, Shukla PR, Pirani A, Moufouma-Okia W, Péan C, Pidcock R, Connors S, Matthews JBR, Chen Y, Zhou X, Gomis MI, Lonnoy E, Maycock T, Tignor M, and Waterfield T (eds.)].

IPCC (2019) Summary for Policymakers. In: IPCC Special Report on the Ocean and Cryosphere in a Changing Climate [Pörtner H-O, Roberts DC, Masson-Delmotte V, Zhai P, Tignor M, Poloczanska E, Mintenbeck K, Alegría A, Nicolai M, Okem A, Petzold J, Rama B, Weyer NM (eds.)]. Cambridge University Press, Cambridge, UK and New York, NY, USA, pp. 3–35. https://doi.org/10.1017/9781009157964.001.

Isa Y, Ikehara N, Yamazato K (1980) Evidence for the occurrence of Ca2+-dependent adenosine triphosphatase in a hermatypic coral, Acropora hebes (Dana). Sesoko Mar Sci Lab Tech Rep 7:19–25

Jokiel PL (2011) Ocean acidification and control of reef coral calcification by boundary layer limitation of proton flux. Bull Mar Sci 87:639–657. https://doi.org/10.5343/bms.2010.1107

Kaniewska P, Campbell PR, Kline DI, Rodriguez-Lanetty M, Miller DJ, Dove S, Hoegh-Guldberg O (2012) Major cellular and physiological impacts of ocean acidification on a reef building coral. PLoS ONE 7:e34659. https://doi.org/10.1371/journal.pone.0034659

Koch M, Bowes G, Ross C, Zhang X (2013) Climate change and ocean acidification effects on seagrasses and marine macroalgae. Glob Chang Biol 19:103–132. https://doi.org/10.1111/j.1365-2486.2012.02791.x

Kroeker KJ, Kordas RL, Crim R, Hendriks IE, Ramajo L, Singh GS, Duarte CM, Gattuso J (2013a) Impacts of ocean acidification on marine organisms: quantifying sensitivities and interaction with warming. Glob Chang Biol 19:1884–1896. https://doi.org/10.1111/gcb.12179

Kroeker KJ, Micheli F, Gambi MC (2013b) Ocean acidification causes ecosystem shifts via altered competitive interactions. Nat Clim Chang 3:156–159. https://doi.org/10.1038/nclimate1680

Krueger T, Horwitz N, Bodin J, Giovani ME, Escrig S, Meibom A, Fine M (2017) Common reef-building coral in the northern red sea resistant to elevated temperature and acidification. R Soc Open Sci 4:170038. https://doi.org/10.1098/rsos.170038

Krueger T, Bodin J, Horwitz N, Loussert-Fonta C, Sakr A, Escrig S, Fine M, Meibom A (2018) Temperature and feeding induce tissue level changes in autotrophic and heterotrophic nutrient allocation in the coral symbiosis—A NanoSIMS study. Sci Rep 8:12710. https://doi.org/10.1038/s41598-018-31094-1

Kurihara H, Watanabe A, Tsugi A et al (2021) Potential local adaptation of corals at acidified and warmed Nikko Bay. Palau Sci Rep 11:11192. https://doi.org/10.1038/s41598-021-90614-8

Lee T-Y (2021) Lactate: a multifunctional signaling molecule. Yeungnam Univ J Med 38:183–193. https://doi.org/10.12701/yujm.2020.00892

Lesser MP, Slattery M, Macartney KJ (2022) Using stable isotope analyses to assess the trophic ecology of scleractinian corals. Oceans 3:527–546. https://doi.org/10.3390/oceans3040035

Leung JYS, Zhang S, Connell SD (2022) Is ocean acidification really a threat to marine calcifiers? a systematic review and meta-analysis of 980+ studies spanning two decades. Small. https://doi.org/10.1002/smll.202107407

Lewis E, Wallace D, Allison LJ (1998) Program developed for CO_2 system calculations. Oak Ridge, TN. https://doi.org/10.2172/639712

Liberti MV, Locasale JW (2016) The warburg effect: how does it benefit cancer cells? Trends Biochem Sci. https://doi.org/10.1016/j.tibs.2015.12.001

Linsley BK, Messier RG, Dunbar RB (1999) Assessing between-colony oxygen isotope variability in the coral Porites lobata at Clipperton Atoll. Coral Reefs 18:13–27. https://doi.org/10.1007/s003380050148

Linsmayer LB, Deheyn DD, Tomanek L, Tresguerres M (2020) Dynamic regulation of coral energy metabolism throughout the diel cycle. Sci Rep 10:19881. https://doi.org/10.1038/s41598-020-76828-2

Loya Y, Sakai K, Yamazato K, Nakano Y, Sambali H, van Woesik R (2001) Coral bleaching: the winners and the losers. Ecol Lett 4:122–131. https://doi.org/10.1046/j.1461-0248.2001.00203.x

Marubini F, Ferrier-Pages C, Cuif JP (2003) Suppression of skeletal growth in scleractinian corals by decreasing ambient carbonation concentration: a cross-family comparison. Proceedings of the Royal Society B: Biological Sciences 270:179–184. https://doi.org/10.1098/rspb.2002.2212

Marcela, Herrera Yi Jin, Liew Alexander, Venn Eric, Tambutté Didier, Zoccola Sylvie, Tambutté Guoxin, Cui Manuel, Aranda (2021) New Insights From Transcriptomic Data Reveal Differential Effects of CO_2 Acidification Stress on Photosynthesis of an Endosymbiotic Dinoflagellate in hospite Frontiers in Microbiology https://doi.org/10.3389/fmicb.2021.666510

Masuko T, Minami A, Iwasaki N, Majima T, Nishimura S-I, Lee YC (2005) Carbohydrate analysis by a phenol–sulfuric acid method

in microplate format. Anal Biochem 339:69–72. https://doi.org/10.1016/j.ab.2004.12.001
McCulloch M, Falter J, Trotter J, Montagna P (2012) Coral resilience to ocean acidification and global warming through pH up-regulation. Nat Clim Chang 2:623–627. https://doi.org/10.1038/nclimate1473
Mclachlan R, Munoz-Garcia A, G Grottoli A (2020). Extraction of Total Soluble Lipid from Ground Coral Samples v1. https://doi.org/10.17504/protocols.io.bc4qiyvw
Mehrbach C, Culberson CH, Hawley JE, Pytkowicx RM (1973) Measurement of the apparent dissociation constants of carbonic acid in seawater at atmospheric pressure 1. Limnol Oceanogr 18(6):897–907
Mollica NR, Guo W, Cohen AL, Huang K-F, Foster GL, Donald HK, Solow AR (2018) Ocean acidification affects coral growth by reducing skeletal density. Proc Natl Acad Sci 115:1754–1759. https://doi.org/10.1073/pnas.1712806115
Mook WG, Bommerson JC, Staverman WH (1974) Carbon isotope fractionation between dissolved bicarbonate and gaseous carbon dioxide. Earth Planet Sci Lett 22:169–176. https://doi.org/10.1016/0012-821X(74)90078-8
Moya A, Huisman L, Ball EE, Hayward DC, Grasso LC, Chua CM, Woo HN, Gattuso J-P, Forêt S, Miller DJ (2012) Whole transcriptome analysis of the coral *Acropora millepora* reveals complex responses to CO_2 -driven acidification during the initiation of calcification. Mol Ecol 21:2440–2454. https://doi.org/10.1111/j.1365-294X.2012.05554.x
Mucci A (1983) The solubility of calcite and aragonite in seawater at various salinities, temperatures, and one atmosphere total pressure. Am J Sci 283:780–799. https://doi.org/10.2475/ajs.283.7.780
Mullarky E, Cantley LC (2015) Diverting Glycolysis to Combat Oxidative Stress. In: Innovative Medicine. Springer Japan, pp. 3–23. https://doi.org/10.1007/978-4-431-55651-0_1
Murphy JWA, Richmond RH (2016) Changes to coral health and metabolic activity under oxygen deprivation. PeerJ 4:e1956. https://doi.org/10.7717/peerj.1956
Muscatine L, Porter JW, Kaplan IR (1989) Resource partitioning by reef corals as from stable isotope composition* I. 513C of zooxanthellae and animal tissue vs depth determined. Marine Biol 100(2):185–193
Muscatine L, Falkowski PG, Porter JW, Dubinsky Z (1984) Fate of Photosynthetic Fixed Carbon in Light- and Shade-Adapted Colonies of the Symbiotic Coral Stylophora pistillata.
Muscatine L (1990) The role of symbiotic algae in carbon and energy flux in reef corals. Coral reefs.
Naguib YMA (2000) A fluorometric method for measurement of oxygen radical-scavenging activity of water-soluble antioxidants. Anal Biochem 284:93–98. https://doi.org/10.1006/abio.2000.4691
Nahon S, Richoux NB, Kolasinski J, Desmalades M, Ferrier Pages C, Lecellier G, Planes S, Berteaux Lecellier V (2013) Spatial and temporal variations in stable carbon (δ13C) and nitrogen (δ15N) isotopic composition of symbiotic scleractinian corals. PLoS ONE 8:e81247. https://doi.org/10.1371/journal.pone.0081247
Orr JC, Fabry VJ, Aumont O, Bopp L, Doney SC, Feely RA, Gnanadesikan A, Gruber N, Ishida A, Joos F, Key RM, Lindsay K, Maier-Reimer E, Matear R, Monfray P, Mouchet A, Najjar RG, Plattner G-K, Rodgers KB, Sabine CL, Sarmiento JL, Schlitzer R, Slater RD, Totterdell IJ, Weirig M-F, Yamanaka Y, Yool A (2005) Anthropogenic ocean acidification over the twenty-first century and its impact on calcifying organisms. Nature 437:681–686. https://doi.org/10.1038/nature04095
Pandolfi JM, Connolly SR, Marshall DJ, Cohen AL (2011) Projecting coral reef futures under global warming and ocean acidification. Science 333:418–422. https://doi.org/10.1126/science.1204794
Pätzold J (1984) Growth rhythms recorded in stable isotopes and density bands in the reef coral Porites lobata (Cebu, Philippines). Coral Reefs 3:87–90. https://doi.org/10.1007/BF00263758
Planes S, Allemand D, Agostini S, Banaigs B, Boissin E, Boss E, Bourdin G, Bowler C, Douville E, Flores JM, Forcioli D, Furla P, Galand PE, Ghiglione J-F, Gilson E, Lombard F, Moulin C, Pesant S, Poulain J, Reynaud S, Romac S, Sullivan MB, Sunagawa S, Thomas OP, Troublé R, de Vargas C, Vega Thurber R, Voolstra CR, Wincker P, Zoccola D (2019) The Tara Pacific expedition—A pan-ecosystemic approach of the "-omics" complexity of coral reef holobionts across the Pacific Ocean. PLoS Biol 17:e3000483. https://doi.org/10.1371/journal.pbio.3000483
Plichon K, Furla P (2024a) Total carbohydrate content for coral samples. protocols.io https://protocols.io/view/total-carbohydrate-content-for-coral-samples-cx56xq9e, https://doi.org/10.17504/protocols.io.36wgq3j4xlk5/v1
Plichon K, Furla P (2024b) Total lipid content analysis for coral samples. protocols.io https://protocols.io/view/total-lipid-content-analysis-for-coral-samples-cxwrxpd6, https://doi.org/10.17504/protocols.io.81wgbx681lpk/v1
Plichon K, Tredez Marion, Roberty S, Canesi M, Beraud E, Douville E, Zoccola D, Gilson E, Reynaud S, Furla P (2024). Coping with ocean acidification: metabolic shifts in Porites corals from the Palau Archipelago. Zenodo. https://doi.org/10.5281/zenodo.14509258
Price JT, McLachlan RH, Jury CP, Toonen RJ, Grottoli AG (2021) Isotopic approaches to estimating the contribution of heterotrophic sources to Hawaiian corals. Limnol Oceanogr 66:2393–2407. https://doi.org/10.1002/lno.11760
Reynaud S, Ferrier-Pagès C, Sambrotto R, Juillet-Leclerc A, Jaubert J, Gattuso J (2002) Effect of feeding on the carbon and oxygen isotopic composition in the tissues and skeleton of the zooxanthellate coral Stylophora pistillata. Mar Ecol Prog Ser 238:81–89. https://doi.org/10.3354/meps238081
Ries JB (2011) A physicochemical framework for interpreting the biological calcification response to CO_2-induced ocean acidification. Geochim Cosmochim Acta 75:4053–4064. https://doi.org/10.1016/j.gca.2011.04.025
Rivera HE, Cohen AL, Thompson JR et al (2022) Palau's warmest reefs harbor thermally tolerant corals that thrive across different habitats. Commun Biol 5:1394. https://doi.org/10.1038/s42003-022-04315-7
Rivest EB, Hofmann GE (2014) Responses of the metabolism of the larvae of Pocillopora damicornis to ocean acidification and warming. PLoS ONE 9:e96172. https://doi.org/10.1371/journal.pone.0096172
Robergs RA, Ghiasvand F, Parker D, Biochemistry DP (2004) Biochemistry of exercise-induced metabolic acidosis. Am J Physiol Regul Integr Comp Physiol. https://doi.org/10.1152/ajpregu.00114.2004
Rodolfo-Metalpa R, Houlbrèque F, Tambutté É, Boisson F, Baggini C, Patti FP, Jeffree R, Fine M, Foggo A, Gattuso J-P, Hall-Spencer JM (2011) Coral and mollusc resistance to ocean acidification adversely affected by warming. Nat Clim Chang 1:308–312. https://doi.org/10.1038/nclimate1200
Roeske CA, O'Leary MH (1985) Carbon isotope effect on carboxylation of ribulose bisphosphate catalyzed by ribulose bisphosphate carboxylase from Rhodospirillum rubrum. Biochemistry 24:1603–1607. https://doi.org/10.1021/bi00328a005
Sassaman C, Mangum CP (1973) Relationship between aerobic and anaerobic metabolism in estuarine anemones. Comp Biochem Physiol A Physiol 44:1313–1319. https://doi.org/10.1016/0300-9629(73)90270-3
Shamberger KEF, Cohen AL, Golbuu Y, McCorkle DC, Lentz SJ, Barkley HC (2014) Diverse coral communities in naturally acidified

waters of a Western Pacific reef. Geophys Res Lett 41:499–504. https://doi.org/10.1002/2013GL058489
Smith A, Cook N, Cook K, Brown R, Woodgett R, Veron J, Saylor V (2021) Field measurements of a massive porites coral at goolboodi (Orpheus Island). Great Barrier Reef Sci Rep 11:15334. https://doi.org/10.1038/s41598-021-94818-w
Spalding C, Finnegan S, Fischer WW (2017) Energetic costs of calcification under ocean acidification. Global Biogeochem Cycles 31:866–877. https://doi.org/10.1002/2016GB005597
Stat M, Pochon X, Cowie R, Gates R (2009) Specificity in communities of Symbiodinium in corals from Johnston Atoll. Mar Ecol Prog Ser 386:83–96. https://doi.org/10.3354/meps08080
Stimson J, Kinzie RA (1991) The temporal pattern and rate of release of zooxanthellae from the reef coral Pocillopora damicornis (Linnaeus) under nitrogen-enrichment and control conditions. J Exp Mar Biol Ecol 153:63–74. https://doi.org/10.1016/S0022-0981(05)80006-1
Suggett DJ, Hall-Spencer JM, Rodolfo-Metalpa R, Boatman TG, Payton R, Tye Pettay D, Johnson VR, Warner ME, Lawson T (2012) Sea anemones may thrive in a high CO_2 world. Glob Chang Biol 18:3015–3025. https://doi.org/10.1111/j.1365-2486.2012.02767.x
Sun Y, Sheng H, Rädecker N, Lan Y, Tong H, Huang L, Jiang L, Diaz-Pulido G, Zou B, Zhang Y, Kao S-J, Qian P-Y, Huang H (2024) Symbiodiniaceae algal symbionts of Pocillopora damicornis larvae provide more carbon to their coral host under elevated levels of acidification and temperature. Commun Biol 7:1528. https://doi.org/10.1038/s42003-024-07203-4
Tambutté E, Allemand D, Zoccola D, Meibom A, Lotto S, Caminiti N, Tambutté S (2007) Observations of the tissue-skeleton interface in the scleractinian coral Stylophora pistillata. Coral Reefs 26:517–529. https://doi.org/10.1007/s00338-007-0263-5
Tambutté S, Holcomb M, Ferrier-Pagès C, Reynaud S, Tambutté É, Zoccola D, Allemand D (2011) Coral biomineralization: From the gene to the environment. J Exp Mar Biol Ecol 408:58–78
Tambutté E, Venn AA, Holcomb M, Segonds N, Techer N, Zoccola D, Allemand D, Tambutté S (2015) Morphological plasticity of the coral skeleton under CO_2-driven seawater acidification. Nat Commun 6:7368. https://doi.org/10.1038/ncomms8368
Tribollet A, Godinot C, Atkinson M, Langdon C (2009) Effects of elevated pCO_2 on dissolution of coral carbonates by microbial euendoliths. Global Biogeochem Cycles. https://doi.org/10.1029/2008GB003286
Tribollet A, Chauvin A, Cuet P (2019) Carbonate dissolution by reef microbial borers: a biogeological process producing alkalinity under different pCO_2 conditions. Facies 65:9. https://doi.org/10.1007/s10347-018-0548-x
van Woesik Peter R, Houk Adelle L, Isechal Jacques W, Steven I, Yimnang V, Golbuu (2012) Climate–change refugia in the sheltered bays of Palau: analogs of future reefs. Abstract Ecology and Evolution 2(10):2474–2484. https://doi.org/10.1002/ece3.2012.2
Venn A, Tambutté E, Holcomb M, Allemand D, Tambutté S (2011) Live Tissue imaging shows reef corals elevate pH under their calcifying tissue relative to seawater. PLoS ONE 6:e20013. https://doi.org/10.1371/journal.pone.0020013
Venn AA, Tambutté E, Caminiti-Segonds N, Techer N, Allemand D, Tambutté S (2019) Effects of light and darkness on pH regulation in three coral species exposed to seawater acidification. Sci Rep 9:2201. https://doi.org/10.1038/s41598-018-38168-0
Venn AA, Tambutté E, Comeau S, Tambutté S (2022) Proton gradients across the coral calcifying cell layer: effects of light, ocean acidification and carbonate chemistry. Front Mar Sci 9:973908. https://doi.org/10.3389/fmars.2022.973908
Ventura P, Jarrold MD, Merle PL, Barnay-Verdier S, Zamoum T, Rodolfo-Metalpa R, Calosi P, Furla P (2016) Resilience to ocean acidification: decreased carbonic anhydrase activity in sea anemones under high pCO_2 conditions. Mar Ecol Prog Ser 559:257–263. https://doi.org/10.3354/meps11916
Vidal-Dupiol J, Zoccola D, Tambutté E, Grunau C, Cosseau C, Smith KM, Freitag M, Dheilly NM, Allemand D, Tambutté S (2013) Genes related to ion-transport and energy production are upregulated in response to CO_2-driven pH decrease in corals: new insights from transcriptome analysis. PLoS ONE 8:e58652. https://doi.org/10.1371/journal.pone.0058652
Wall CB, Fan T-Y, Edmunds PJ (2014) Ocean acidification has no effect on thermal bleaching in the coral Seriatopora caliendrum. Coral Reefs 33:119–130. https://doi.org/10.1007/s00338-013-1085-2
Wall M, Fietzke J, Schmidt GM, Fink A, Hofmann LC, de Beer D, Fabricius KE (2016) Internal pH regulation facilitates in situ long-term acclimation of massive corals to end-of-century carbon dioxide conditions. Sci Rep 6:30688
Wang J-T, Douglas AE (1998) Nitrogen recycling or nitrogen conservation in an alga-invertebrate symbiosis? J Exp Biol 201:2445–2453. https://doi.org/10.1242/jeb.201.16.2445
Warburg O (1925) The metabolism of carcinoma cells. J Cancer Res 9:148–163. https://doi.org/10.1158/jcr.1925.148
Warburg O, Minami S (1923) Versuche an überlebendem carcinomgewebe. Klin Wochenschr 2:776–777. https://doi.org/10.1007/BF01712130
Weis VM, Smith GJ, Muscatine L (1989) A "CO_2 supply" mechanism in zooxanthellate cnidarians: role of carbonic anhydrase. Marine Biol 100(2):195–202
Zoccola D, Tambutté E, Sénégas-Balas F, Michiels J-F, Failla J-P, Jaubert J, Allemand D (1999) Cloning of a calcium channel α1 subunit from the reef-building coral, Stylophora pistillata. Gene 227:157–167. https://doi.org/10.1016/S0378-1119(98)00602-7
Zoccola D, Tambutté E, Kulhanek E, Puverel S, Scimeca J-C, Allemand D, Tambutté S (2004) Molecular cloning and localization of a PMCA P-type calcium ATPase from the coral Stylophora pistillata. Biochimica Et Biophysica Acta (BBA)-Biomembranes 1663:117–126. https://doi.org/10.1016/j.bbamem.2004.02.010
Zoccola D, Innocenti A, Bertucci A, Tambutté E, Supuran CT, Tambutté S (2016) Coral carbonic anhydrases: regulation by ocean acidification. Mar Drugs 14:109. https://doi.org/10.3390/md14060109
Zamoum T, Furla P (2012) Symbiodinium isolation by NaOH treatment Summary Journal of Experimental Biology https://doi.org/10.1242/jeb.074955